TROPOS
Leibniz Institute for
Tropospheric Research

Leibniz-Institut für Troposphärenforschung Permoserstraße 15 D-04318 Leipzig

Prof. Hartmut Herrmann
Head of TROPOS Atmospheric
Chemistry Department
herrmann@tropos.de
phon: +49 341 2717 7024
fax: +49 341 2717 99 7023
Permoserstraße 15
04318 Leipzig
24.07.2020

The Editor
Atmospheric Chemistry and Physics

Submission of revision for the Atmospheric Chemistry and Physics "Major Revision" manuscript 'Role of the dew water on the ground surface in HONO distribution: a case measurement in Melpitz' (MS No.: acp-2019-1088) by by Yangang Ren, Bastian Stieger, Gerald Spindler, Benoit Grosselin, Abdelwahid Mellouki, Thomas Tuch, Alfred Wiedensohler and Hartmut Herrmann

Dear Editor,

Please find attached here our response to the reviewer comments for the manuscript mentioned above together with its revised versions of the manuscript and supplement. We would like to thank both of the reviewers for all of their valuable and insightful comments to improve the manuscript. We have carefully considered all the reviewer comments and revised the manuscript accordingly. Below, we provide responses to the comments in blue, with changes made in blue in the manuscript.

Sincerely yours,

Prof. Dr. H. Herrmann
Professor of Atmospheric Chemistry
Head of TROPOS Atmospheric Chemistry Department

Referee #1

The authors gratefully thank the reviewer for the comments and suggestions. We have revised our manuscript according to the reviewer's suggestions and comments. **All the changes and responses to the reviewers' comments are listed below point-by-point in blue according to a new line numbering in the revised manuscript. The major changes are highlighted with blue in the revised manuscript.**

Comments to the revised manuscript by Ren et al.

In their revised manuscript Ren et al. considered most concerns of the two reviewers. However, I still have three major concerns (and some minor) which should be considered before publication in ACP.

Major Concerns:

1) Calculated NO2 uptake coefficients for particles surfaces (page 12, section 4.2.2):
In their revised manuscript Ren et al. now use the correct equation for converting the uptake coefficient into a first order rate coefficient (see Eq. 3). But the calculated theoretical uptake coefficients to explain night-time formation of HONO on particles are still unrealistically low (1.5x10^-6 – 1.9 x10-5, see line 414) in contrast to former studies who determined values of 10^-4 and larger and from which HONO formation on particles could be easily excluded (there is no such fast NO2 kinetics known from lab studies…). Reason for the low number of the authors (with which the HONO formation could be explained!? in contrast to the author's conclusion…) is the unrealistically high S/V(a) ratio of 9x10^-3 m^2 m^-3, which they gave only in the response letter (page 9) and which should be also specified in the manuscript.
I found S/V(a) values of 3x10^-4 m^2 m^-3 for heavily urban conditions (Finlayson-Pitts and Pitts textbook) and a value of ca. 200 um^2 m^-3 for Beijing (ACP, 17, 2017, 12327) which can be converted into 2x10^-4 m^2 m^-3. Thus, in Melpitz (low pollution) the aerosol surface density should be 45 times higher (!) than in Beijing (polluted)? The authors should check their data again. If the lower S/V ratio from Beijing was used, the theoretical uptake coefficient would be 45 times higher (and for Melpitz even more…) bringing the theoretical uptake coefficient into a reasonable range (10^-4) similar to former studies and thus confirming the author's argument (no HONO formation on particles…)!

Response: The particle surface density S/V_a was calculated using the following equation: $\sum_l^u(\pi D_\rho^2 n)$ by assuming the particles are in spherical shape where l and u are the lower and upper channel boundary, respectively. D_ρ is the particle diameter (channel midpoint) and n is number weighted concentration per channel. However, unfortunately, the particle number n was confused with $dN/d\log D_\rho$. We are sorry for this mistake and thanks to the reviewer for

recognizing it. Accordingly, S/V_a was recalculated as (5.1-9.9)$\times10^{-4}$ m^2 m^{-3}, was further corrected with a hygroscopic factor $f(RH)=1+a\times(RH/100)^b$ (empirical factors a and b were set to 2.06 and 3.6, respectively) resulting in (0.6-1.9) $\times10^{-3}$ m^2 m^{-3}. This value now relates much more reasonable to S/V ratios reported in the literature, e.g. for Beijing as 0.2-3.4$\times10^{-3}$ m^2 m^{-3} (Liu et al., 2014, Wang et al., 2016). The value of ca. 2×10^{-4} m^2 m^{-3} reported by Cai et al., (2017) was for observed new particle formation (NPF) events in Beijing and the value ranged from 3.5×10^{-4} m^2 m^{-3} to 1.1×10^{-3} m^2 m^{-3} for non-NPF event. Finally, the calculated $\gamma_{NO2\rightarrow HONO\_a}$ varied from 2.8×10^{-5} to 3.8×10^{-4} with a mean value of (1.7±1.0) $\times10^{-4}$ in this work. All values have now been updated in the manuscript as:

Line 417-419, "The particle surface density S_a was calculated as (5.1-9.9) $\times10^{-4}$ m^2 m^{-3} from the particle size distribution …. The particle surface density S_a was further corrected to be (0.6-1.9) $\times10^{-3}$ m^2 m^{-3} …"
Line 431-435, "the calculated $\gamma_{NO2\rightarrow HONO\_a}$ varied from 2.8×10^{-5} to 3.8×10^{-4} with a mean value of (1.7±1.0) $\times10^{-4}$. This theoretical uptake coefficient falls into a reasonable range of 10^{-6} - 10^{-4} similar to former studies (Kleffmann et al., 1998, Kurtenbach et al., 2001, Wong et al., 2011, VandenBoer et al., 2013)."

2) Plot of k(het) against the inverse wind speed:
In response to my concern from the first review the authors have added now a new plot (Fig. S8b), which I recommended to confirm that HONO formation takes place on the ground and not on aerosols. First, now the authors have added this plot/argument in section 4.2.3 (HONO deposition on the ground) where it makes no sense!? Second, in their plot they not used the same data by which the values of k(het) were determined (see Table 3 and Fig S4). For k(het) the authors correctly used only the first initial increase of HONO/NO2, which was not too much affected by HONO deposition (Tab. 3). In contrast for Figure S8b data from all the night is evaluated (18:00-4:00), which is significantly affected by the HONO deposition making k(het) significantly lower than for data in Tab. 3. Thus, the same plot should be repeated for the data from Tab. 3 and then should be plotted against the inverse average wind speed for the same time period (apples and apples…).

Response: The first version of our plot of $HONO/NO_2$ against wind speed was presented in the manuscript in the ACPD 'Interactive Discussion stage' (as below Figure R1) and we discussed the impact of wind speed on NO_2-to-HONO conversion and HONO deposition. Hence, we put the plot in the section 4.2.3 (HONO deposition on the ground). As the reviewer suggested in the first round of review, we plotted the $k_{(het)}$ against the inverse wind speed (previous Figure S8b, now as Figure S8a) and kept it in the section 4.2.3 to discuss the same concern because it also included one data of observation "HONO peak observed at 0:00-2:00 (UTC) of April 25th (Figure 5) in line 306".

Our previous Figure S8b (now Figure S8a) includes the data of Tab. 3. Six conditions were selected to calculate the NO_2-HONO frequency following the criteria of Li et al. 2018, line 389) while four conditions were not considered in Tab. 3 because of their low R^2 (<0.4). All these k(het) values were calculated using only the first initial increase of $HONO/NO_2$. The previous Figure S8b (now Figure S8a) also included one data of observation "HONO peak observed at 0:00-2:00 (UTC) of April 25th (Figure 5) in line 306". This data shows a high k(het) of 0.06 h^{-1} for high wind speed of 4.08 m s^{-1}. It is assumed that the evaporation of dew droplets resulted in the temporary HONO peak.

In the revised version, we plot the data from Tab. 3 and also one data point according to the second set of observation (mentioned in section 3.3 and Figure 5) against the inverse average wind speed as shown in Figure S8a and move the plot to section 4.2.2 'Relative importance of particle and ground surface in nocturnal HONO production' as:

Line 466-474, "In addition, the relationship of NO_2-HONO conversion frequency (k_{het} presented in Table 3) with the inverse of wind speed is illustrated in Figure S8a. As indicated in Figure S8a, wind speed was predominantly less than 3 m s^{-1} during the field campaign period in Melpitz. High conversion frequency of NO_2-to-HONO mostly happened when wind speed was less than 1 m s^{-1}, which confirms that HONO formation mainly takes place on the ground. However, one point (in blue in Figure S8a) showed highest NO_2-HONO conversion frequency (k_{het}) when wind speed was ca. 4 m s^{-1} according to the second set of observation mentioned in section 3.3 and Figure 5. The likely reason for the temporary HONO peak is the dew droplet evaporation after increasing wind speed."

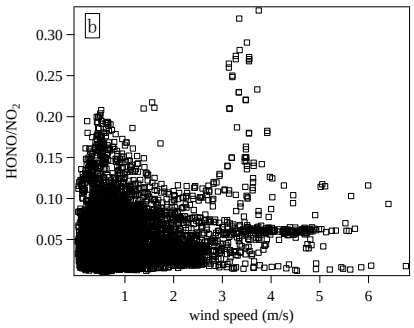

Figure R1. Scatter plot of $HONO/NO_2$ against wind speed in the time interval of 18:00-04:00 (UTC).

3) Explanation of the morning HONO peaks by dew water nitrite.

The quantitative calculation of the peak HONO by evaporation of dew water nitrite is not correct and too simple. First, why do the authors not simply take F(NO2-) in Eq. 16 but multiply that by 2 and by the LAI (x6), i.e. why do they used a 12 times higher values than measured? If dew is condensing on the ground the volume of the water is limited by the amount of humid air which gets into contact with the cold surfaces but it is not limited by the

surface area!? Thus, on any higher surface area of plants (compared to the geometric surface of their glass plates…) the total dew volume would be the same! Thus, they should not use the enhancement factor of 12 here (2x6).

Response: There are multiple kinds of environmental surfaces as well as smaller surfaces may be more effective in collecting dew (Kotzen 2015). As mentioned by Wentworth et al., (2016), the volume of dew (V_{dew}) obtained from the collector is not necessarily representative of V_{dew} that forms naturally on the grassland canopy because of their different cold contacted surface area with humid air. The V_{dew} could also be affected by the collector materials (del Campo et al., 2006, Guan et al., 2014, Kotzen 2015), they noted that the single walled tree shelter was a better condensation collector as it had 40% more available surface area to collect dew due to its corrugations on one side. Kotzen (2015) concluded that the main ways to enhance dew formation and collection is to increase surface area and facilitating maximum radiative cooling to the open sky based on the testing of nearly two hundred materials.
In this work, we collected the dew water using a glass plate and the NO_2^- concentration **per m^2 of the sampler surface** (F_{NO2-}) was calculated from the following equation:

$$F_{NO2-} = \frac{[NO_2^-]\times V_{dew}}{S\times 1000} \quad \text{(Eq. 2)}$$

Here, $[NO_2^-]$ is the sample concentration in µg L^{-1}, V_{dew} is the sample volume in ml of the glass sampler, S is the surface area of the glass sampler 1.5 m^2 as explained in line 353-358.
Then the hypothetical morning HONO mixing ratio (pptv) due to the complete dew water evaporation could be estimated from the following equation by taking the measured dew nitrite and the mixing layer height:

$$[HONO] = \frac{2\times LAI\times F_{NO2-}}{mixing\ height} \quad \text{(previous Eq. 16)}$$

In which the complete Eq.16 should be:

$$[HONO] = \frac{2\times LAI\times S\times F_{NO2-}}{H\times S} = \frac{2\times LAI\times F_{NO2-}}{H}$$

F_{NO2}^- is the NO_2^- concentration per m^2 of the glass sampler surface, S represents the flat ground surface (analog to the surface area of the glass sampler). But the V_{dew} on the glass sampler could be enhanced due to the larger cold surfaces from grass which can get in contact with humid air than the plat glass sampler. This enhancement factor was calculated as 2 ×LAI to take the vegetation-covered areas on the ground and the areas on the both sides of the leaves into account. This is why we used a 12 times higher values than measured F_{NO2}^-.
Accordingly, we modified Equation 16 to clarify in line 643-651:

"$$[HONO] = \frac{\alpha\times S_g\times F_{NO2-}}{H\times S_g} = \frac{\alpha\times F_{NO2-}}{H} \quad \text{(Eq. 17)}$$

F_{NO2}^- is the NO_2^- concentration per m^2 of the glass sampler surface, S_g represents the surface area of the flat ground (analog to the surface area of the glass sampler), α is the enhanced factor for V_{dew} (dew water sample volume of the glass sampler in Eq.2) due to the larger cold

surfaces from grass which can get in contact with humid air than the flat glass sampler. α was calculated as $2 \times$ LAI to take the areas on the both sides of the leaves and the vegetation-covered areas on the ground into account. Regarding the grass height during the dew measurements (~30cm) that is approximately the height in April 2018 and May 2019, we used a factor of 6 for LAI.

Second, the dew evaporation took place during early daytime when HONO photolysis is already significant. At 7:00 (HONO peak time) J(HONO) will be approximately half of the noon time value and thus evaporated HONO is significantly lost by photolysis over its evaporation time period (ca. 3 h, see Fig. 6). This problem can be only solved by a simple model including HONO production (by dew nitrite evaporation) and loss by photolysis. Since I do not have the (J(HONO) data I simply used a linear increase of J(HONO) from zero at 4:00 to 5x10^-4 s^-1 (at 7:00, see Fig. 6) in a model and used the maximum F(NO2-) of 8 ug m^-2 (1x10^17 HONO m^-2). For a reasonable mixing height of 100 m this can be converted into a HONO concentration of 42 ppt. But the production term over a time period of 3 hours (see Fig 6, 4:00 – 7:00) is only P(HONO from dew) = 0.004 ppt/s (42ppt/10800s). Now if I use the model including also HONO photolysis (see above) the peak HONO concentration after ca. 2 h (then HONO is decreasing again by increasing photolytic loss…) is only 14 ppt (and not 42…). This value is much lower than the experimental increase of HONO during the morning peak of ca. 450 ppt shown in Figure 6. In addition, the average dew nitrite concentration was not 8 ug/m2 but 3.5 ug/m2 (see table 2). Thus, the nitrite is by far not enough to explain the HONO morning peaks.
Here one argument could be the dew measurements one year after the HONO measurements (see my first review) comparing apples and oranges. But maybe also other sources are still not correctly considered here.

Response: Firstly, we need to note that, higher F_{NO2^-} was obtained on May 11th where dew water was not frozen as shown in Table 2. On other days (May 8th, May 13th and May 14th) frozen dew water was observed, which likely inhibited HONO to dissolve. Hence, these frozen samples were not considered in this paper. On May 11th, the final F_{NO2}^- could be obtained by averaging F_{NO2}^- of the sum (9.43 μg m^{-2}) of the first and third sample with the second sample (6.40 μg m^{-2}) on 11th May resulting in 7.91±2.14 μg m^{-2}. We explained this in line 358-364. Hence, the overall concentration increase from this source would be 453 pptv if dissolved HONO was released into the overlying air column of 100 m mixing height.
Secondly, we agree with the reviewer that our quantitative calculation of the HONO peak by dew water evaporation is simple not taking into account the HONO photolysis. Considering the HONO photolysis using the photolysis rate of HONO from the TUV model, a HONO maximum of 211 pptv would be released by dew evaporation for a mixing height of 100 m at 7:00 UTC after the process started at 4:00 UTC (Figure R2). This would account for ~30% of

the observed HONO morning peak in Figure 6. This low percentage might be a result of the different sampling time of dew measurement compared with HONO measurement. Although the above calculations may be well simplified, the results do suggest that the release of the deposited HONO on wet/moist canopy surfaces may contribute to the morning HONO concentrations right after dew evaporation. Further research is needed to quantify exactly the amount of released HONO on the atmospheric HONO concentrations.

Following this revision, we have modified the description in line 653-666, "Hence, the overall concentration increase from this source would be 2264±612, 1132±306, 453±122, 226±61 and 76±20 pptv, respectively, if deposited HONO released into the overlying air column for a mixing height of 20, 40, 100, 200 and 600 m. Since the released HONO was subjected to photolysis, using a J_{HONO} from TUV model scaled by global radiation (section 2.7), a maximum [HONO] of 1053±45, 527±22, 211±9, 105±4 and 35±1 pptv for the mixing height 20, 40, 100, 200 and 600 m, respectively, would be contributed from the surface nitrite release at 7:00 UTC after the process started from 4:00 UTC. For a reasonable 100 m mixing height, this would account for ~30% of the observed HONO morning peak in Figure 6 and this low percentage might be a result of the different sampling time of dew measurement compared with HONO measurement. Although the above calculations may be well simplified, the results do suggest that the release of the deposited HONO on wet/moist canopy surfaces may contribute to the morning HONO concentrations in the overlying atmosphere right after dew evaporation."

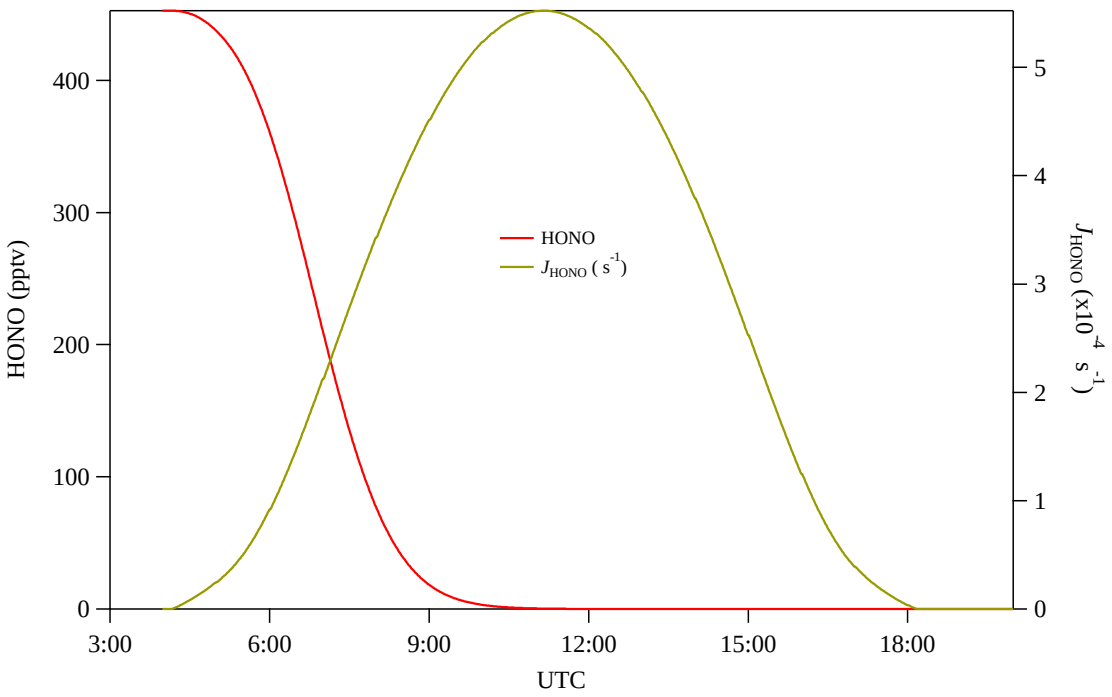

Figure R2. Plot of releasing evolution of deposited HONO subjected to it photolysis from 4:00 UTC using the equation: $[HONO]_t=[HONO]_0 \times \exp(-J_{HONO} \times t)$. $[HONO]_0$ and $[HONO]_t$ are HONO concentration at time 0 and time t (60 s in this case). The $[HONO]_0$ at 4:00 UTC

was calculated from Eq. 16 by assuming all the deposited HONO was released.

Specific Concerns:

The following concerns are listed in the order how they appear in the manuscript.
Lines 48-49: either use an alphabetic or chronologic order of the references.

Response: We use an alphabetic order of the references for all the manuscript.

Sections 2.2 and 2.3
Please unify the units used for both instruments (e.g. detection limit in ug/m3 or ppt) for comparison

Response: We changed the detection limit of MARGA to 10 pptv in Line 148.

Section 2.7:
Please specify that the clear sky J-values by the TUV model were scaled by the measured global radiation, see my first review!

Response: We specify that the clear sky J-values by the TUV model were scaled by the measured global radiation in Line 246.

Line 234-235: you should not compare high time resolution data with the one hour averaged MARGA data, delete the sentence, that is trivial…

Response: We modified the sentence "The hourly HONO mixing ratio obtained from MARGA with the 30 seconds and hourly averaged HONO mixing ratios from LOPAP are shown in Figure 1a and 1b, respectively" in line 252-253.

Line 263: Should be accuracy and not precision. The precision of the data shown in the intercomparison is much higher than the 90 % difference.

Response: We changed the "precision" to "accuracy" in line 278.

Line 295: Should be "the early morning variation trend", since the statement is only true for the first three daytime hours and not for whole diurnal data!

Response: We changed the "diurnal" to "early morning" in line 309.

Line 309: Where do I find argument (a)? The conclusion from Sörgel et al.?

Response: We modified the sentence to make it clear, "As reported by Stemmler et al., (2006), the photosensitized NO_2 on humic acid could act as a source of HONO during the daytime. It was expected that the photosensitized NO_2 on humic acid might lead to a HONO morning peak within hypothesis (b)" in line 320-323.

Line 313-316: The reason for the similar increase of HONO and NO2 is the variation of the vertical mixing increasing the level of all near ground emitted of formed species. Radon would show the same behavior…

Response: We changed the sentence to "… This could be explained by the variation of the vertical mixing increasing the level of all near ground emitted of formed species or the heterogeneous conversion of NO_2 to HONO during nighttime and will be discussed in Section 4." in line 329-332.

Lines 341-348: I would recommend using the average dew nitrite (3.5+-3 ug/m2), since dew and HONO data are from different campaigns… And later I would also use the average HONO data (see Fig. 4) for comparison and not a single day (see Fig. 6).

Response: As we explained in line 358-364, "dew water was frozen until 1 hour after sunrise on May 8th, 13th and 14th 2019 but not on May 11th 2019", which likely inhibited HONO to dissolve. This frost phenomenon was not found during the HONO measurement campaign in 2018. Hence we used value of 7.91±2.14 μg m^{-2} on 11th May for the following calculation and discussion. Exactly both Figure 4 and Figure 6 are the average HONO data, but the previous Figure 4 was included two sets of observation in Figure 5, which should be excluded from the average calculation. In this version, we correct the calculation and update the Figure 4.

Line 370-371: Have the authors subtracted 0.3 % from the experimental HONO/NO2 data? By the way in Kurtenbach et al. HONO/NOx was determined.

Response: As defined in Kurtenbach et al., (2001) and other studies like in Li et al., (2018), the $HONO/NO_X$ ratio was usually chosen to derive the emission factor of HONO in the freshly emitted plumes. Here, we firstly used this emission factor to correct the HONO concentration, then using this corrected HONO concentration to calculate k_{het} from the least linear regression for $[HONO]/[NO_2]$ ratios against time, but not directly subtract 0.3% from the $HONO/NO_2$ ratio.

Line 387-388, we modified the sentence to be "Then in this work, a low emission factor of 0.3% was used to correct the directly HONO emission from vehicles (Kurtenbach et al., 2001)

to result a $[HONO]_{corr}$" to make it clear that "the authors subtracted 0.3 % from directly HONO emission from the NO_2-HONO conversion".

Line 397-399: No, as I already mentioned in my first review, the main reason is the different time periods considered (here only initial increase for the first 2 evening hours in contrast to other studies, where often the whole night was considered and for which parallel deposition leads to smaller values of k(het)).

Response: Because of the increasing role of HONO sink in the second half of night, as mentioned in the rural site studies of Alicke et al., (2003), Li et al., (2012), Acker and Möller (2007) and urban site study of Alicke et al., (2002), Wang et al., (2017), Acker and Möller (2007), the authors restricted the analysis of k_{het} to the time frame from 18:00 to 24:00 like our work, so the argument of "This could be ascribed to the higher S/V surface in the rural site because of the high leaf area index (LAI, m^2/m^2) compared to an urban and might have enhanced the heterogeneous NO_2-HONO conversion." could be right. However, we changed the sentence to be "The higher value may suggest that a more efficient heterogeneous conversion from NO_2 to HONO is present in rural sites than in urban sites" in line 413-414.

Section 4.2.2: Please specify the S/V(a) used

Response: We specified the S/V(a) in line 417-421.

Equation 3: Please specify that you considered a 100 % HONO yield here (NO2+Org/soot/etc., see my first review).

Response: We already mentioned in line 430-431 "If the entire HONO formation was taking place on the particle surface…", here we add another sentence in line 425-426 "by considering 100% HONO yield on the particle surface (NO_2+Org/soot/etc)" to make it clear.

Equation 4: Please specify that you considered a 50 % HONO yield here (2 NO2 + H2O, see my first review).

Response: We clarified it in line 443 "by considering a 50% HONO yield from reaction 2a".

Line 443-447: Here you find exactly the argument for my major concern 1)…

Response: We thanks the reviewer for the insightful point here, we modified the argument in line 461-465 "It should be noted that the obtained NO_2 uptake coefficient on the ground surface is lower than the reactive surface provided by aerosols, but as the S/V ratio of

particles is typically orders of magnitude lower than for ground surfaces, it is suggested that the heterogeneous reactions of NO_2 on ground surface may play a dominant role for the nighttime HONO formation."

Line 503: Should be "… speed is smaller than …" In contrast to what is used here also Rb is depending on the wind speed (see e.g. VDI3782) and the lower the WS the larger is the quasi-laminar layer on the surfaces. Thus transport limitation gets important at low WS.

Response: We changed the sentence in line 523 as the reviewer suggested. Also we mentioned the transport limitation at low WS in line 520-521 "the HONO uptake will be transport-limited if the real uptake coefficients are $\geq 2.8\times10^{-4}$ and wind speed was less than 0.5 m s^{-1}".

Line 593: The upper limit is not given in Stemmler et al., 2006 and this study is not considering aerosol but bulk surfaces?

Response: We changed the citation and decide to use the same value of 2.0×10^{-5} for the aerosol and ground surface as the literature (Zhang et al., 2016). The sentence was modified in line 606-607 "Here the γ_a and γ_g are the light-enhanced NO_2 uptake coefficient of 2.0×10^{-5} (Zhang et al., 2016) on both of the aerosol surface and ground surface, respectively." The according Figure 6 was also updated.

Line 611-612: If k(emission) is determined from the experimental data, it is trivial that the model is doing an excellent job… But the values cannot be explained by the dew nitrite, see major concern 3)

Response: We thank the reviewer for this comment. As discussed in line 618-626, we defined a temporary HONO emission from dew water $k_{emission}$ related to RH using experimental and model result, which provide us a possibility to model the HONO emission from dew evaporation not only in this work but also for other studies in the future. As we already mentioned in the major concern 3, the HONO emission could not be fully explained by the dew measurement mainly due to the different sampling period for HONO and dew measurement. And a future simultaneously HONO and dew measurement could be planned.

Line 639: From where is that number (1400 ppt). In figure 6 (one day) the delta is ca. 450 ppt for the avarge campaign (Fig. 4a) it is ca. 300 ppt…?

Response: We are sorry for the confusion. Because the time of HONO morning peak was different within each day (Figure 2), so we averaged these morning peak value as 1400 pptv.

Both Figure 4 and Figure 6 show time averaged values. We updated them in this version to make it clear. Hence, we modified the sentence in line 660-663 "For a reasonable 100 m mixing height, this would account for ~30% of the observed HONO morning peak in Figure 6. This low percentage might be a result of the different sampling time of dew measurement compared with HONO measurement".

Line 668: It is J(O1D) from the TUV model scaled by the global radiation…

Response: We clarified it in line 694.

Line 664-665: No not the diurnal cycle of the mixing ratio, that is different by 90%! You mean the relative shape of the diurnal data…

Response: We mean that even the HONO mixing ratio measured by MARGA was higher than LOPAP, we also present the diurnal cycle from MARGA measurement in this work. Here we delete the sentence "However, the diurnal cycles of HONO mixing ratio were captured by both instruments" to make it clear.

Line 687: It is the maximum (…) value; on average it is 3.5ug/m2.

Response: We mentioned the "…maximum…" in line 711.

Line 688: Change the numbers (14 ppt in my example…) and it should be e.g. 1230+-160…

Response: We changed the numbers in line 712-715 "under consideration of photolytical losses and homogeneous mixing, the maximum contribution to the HONO morning peak from dew water evaporation could be calculated and ranged from 1053±45 to 35±1 pptv for mixing height of 20 to 600 m, respectively."

Line 695: From where is that number (970 ppt)? (see first version…)

Response: The total deposited HONO (in pptv) on the ground surface was assumed same as the total night-time HONO loss of 970±730 pptv (6 h), calculated by integrating L_{HONO} from 22:00 to 4:00 (UTC) from the nighttime measurement. We are sorry for the mistake. We should correct it as "0.16±0.12 ppbv h^{-1}" in the first version (the same value in the abstract), here we correct it in line 721.

Line 706: Should be minus(!) 0.016…(inverse correlation…)

Response: As defined in Eq. 14: $k_{emission} = \frac{d(\frac{HONO_{unknown}}{99.5-RH})}{dt} = \frac{\frac{HONO_{unknown}}{99.5-RH}(t_2) - \frac{HONO_{unknown}}{99.5-RH}(t_1)}{(t_2 - t_1)}$, here $k_{emission}$ has a positive relationship with (99.5-RH).

I did not check the references…

Response: We checked the references carefully.

Figure 4: Please add a plot of J(HONO) to check the photolytic loss, see major concern.

Response: The plot of J_{HONO} was added in Figure 4a.

Figure 8: In the legend it should be P(HONO->OH) and P(O3->OH), it is not the production of O3 but of OH… In addition how can the production of OH by HONO photolysis be negative? The term by HONO + OH is normally not significant?

Response: We changed the P_{HONO} and P_{O3} to $P_{HONO->OH}$ and $P_{O3->OH}$, respectively, in Figure 8 and also in section 4.3.4.

As we defined in section 4.3.4, the net rate of OH production from HONO photolysis ($P_{HONO->OH}$) was calculated from Eq. 17:

$P_{HONO->OH} = J_{HONO}[HONO] - k_{3a}[NO][OH] - k_9[HONO][OH]$

Where the consumption of OH by its reaction with NO and HONO was also considered. Hence, the net OH production rate in the early morning is negative as shown in Figure 8. And the term of HONO+NO could be important in the early morning but become less after the photolysis of HONO was strong.

References:

Acker, K. and Möller, D., 2007. Corrigendum to: Atmospheric variation of nitrous acid at different sites in Europe. Environ. Chem. 4(5), 364-364.

Alicke, B., Geyer, A., Hofzumahaus, A., Holland, F., Konrad, S., Pätz, H.W., Schäfer, J., Stutz, J., Volz-Thomas, A. and Platt, U., 2003. OH formation by HONO photolysis during the BERLIOZ experiment. J. Geophys. Res. Atmos. 108(D4), 8247.

Alicke, B., Platt, U. and Stutz, J., 2002. Impact of nitrous acid photolysis on the total hydroxyl radical budget during the Limitation of Oxidant Production/Pianura Padana Produzione di Ozono study in Milan. J. Geophys. Res. Atmos. 107(D22), 8196.

Cai, R., Yang, D., Fu, Y., Wang, X., Li, X., Ma, Y., Hao, J., Zheng, J. and Jiang, J., 2017. Aerosol surface area concentration: a governing factor in new particle formation in Beijing. Atmos. Chem. Phys. 17(20), 12327-12340.

del Campo, A.D., Navarro, R.M., Aguilella, A. and González, E., 2006. Effect of tree shelter design on water condensation and run-off and its potential benefit for reforestation establishment in semiarid climates. For. Ecol. Manag. 235(1), 107-115.

Guan, H., Sebben, M. and Bennett, J., 2014. Radiative- and artificial-cooling enhanced dew collection in a coastal area of South Australia. Urban Water Journal 11(3), 175-184.

Kleffmann, J., Becker, K.H. and Wiesen, P., 1998. Heterogeneous NO_2 conversion processes on acid surfaces: Possible atmospheric implications. Atmos. Environ. 32(16), 2721-2729.

Kotzen, B., 2015. Innovation and evolution of forms and materials for maximising dew collection. Ecocycles 1(1), 39-50.

Kurtenbach, R., Becker, K.H., Gomes, J.A.G., Kleffmann, J., Lörzer, J.C., Spittler, M., Wiesen, P., Ackermann, R., Geyer, A. and Platt, U., 2001. Investigations of emissions and heterogeneous formation of HONO in a road traffic tunnel. Atmos. Environ. 35(20), 3385-3394.

Li, D., Xue, L., Wen, L., Wang, X., Chen, T., Mellouki, A., Chen, J. and Wang, W., 2018. Characteristics and sources of nitrous acid in an urban atmosphere of northern China: Results from 1-yr continuous observations. Atmos. Environ. 182, 296-306.

Li, X., Brauers, T., Häseler, R., Bohn, B., Fuchs, H., Hofzumahaus, A., Holland, F., Lou, S., Lu, K.D., Rohrer, F., Hu, M., Zeng, L.M., Zhang, Y.H., Garland, R.M., Su, H., Nowak, A., Wiedensohler, A., Takegawa, N., Shao, M. and Wahner, A., 2012. Exploring the atmospheric chemistry of nitrous acid (HONO) at a rural site in Southern China. Atmos. Chem. Phys. 12(3), 1497-1513.

Liu, Z., Wang, Y., Costabile, F., Amoroso, A., Zhao, C., Huey, L.G., Stickel, R., Liao, J. and Zhu, T., 2014. Evidence of Aerosols as a Media for Rapid Daytime HONO Production over China. Environmental Science & Technology 48(24), 14386-14391.

Stemmler, K., Ammann, M., Donders, C., Kleffmann, J. and George, C., 2006. Photosensitized reduction of nitrogen dioxide on humic acid as a source of nitrous acid. Nature 440, 195.

VandenBoer, T.C., Brown, S.S., Murphy, J.G., Keene, W.C., Young, C.J., Pszenny, A.A.P., Kim, S., Warneke, C., de Gouw, J.A., Maben, J.R., Wagner, N.L., Riedel, T.P., Thornton, J.A., Wolfe, D.E., Dubé, W.P., Öztürk, F., Brock, C.A., Grossberg, N., Lefer, B., Lerner, B., Middlebrook, A.M. and Roberts, J.M., 2013. Understanding the role of the ground surface in HONO vertical structure: High resolution vertical profiles during NACHTT-11. J. Geophys.

Res. Atmos. 118(17), 10,155-110,171.
Wang, G., Zhang, R., Gomez, M.E., Yang, L., Levy Zamora, M., Hu, M., Lin, Y., Peng, J., Guo, S., Meng, J., Li, J., Cheng, C., Hu, T., Ren, Y., Wang, Y., Gao, J., Cao, J., An, Z., Zhou, W., Li, G., Wang, J., Tian, P., Marrero-Ortiz, W., Secrest, J., Du, Z., Zheng, J., Shang, D., Zeng, L., Shao, M., Wang, W., Huang, Y., Wang, Y., Zhu, Y., Li, Y., Hu, J., Pan, B., Cai, L., Cheng, Y., Ji, Y., Zhang, F., Rosenfeld, D., Liss, P.S., Duce, R.A., Kolb, C.E. and Molina, M.J., 2016. Persistent sulfate formation from London Fog to Chinese haze. Proceedings of the National Academy of Sciences 113(48), 13630-13635.
Wang, J., Zhang, X., Guo, J., Wang, Z. and Zhang, M., 2017. Observation of nitrous acid (HONO) in Beijing, China: Seasonal variation, nocturnal formation and daytime budget. Sci. Total Environ. 587, 350-359.
Wentworth, G.R., Murphy, J.G., Benedict, K.B., Bangs, E.J. and Collett Jr., J.L., 2016. The role of dew as a night-time reservoir and morning source for atmospheric ammonia. Atmos. Chem. Phys. 16(11), 7435-7449.
Wong, K.W., Oh, H.-J., Lefer, B.L., Rappenglück, B. and Stutz, J., 2011. Vertical profiles of nitrous acid in the nocturnal urban atmosphere of Houston, TX. Atmos. Chem. Phys. 11(8), 3595-3609.
Zhang, L., Wang, T., Zhang, Q., Zheng, J., Xu, Z. and Lv, M., 2016. Potential sources of nitrous acid (HONO) and their impacts on ozone: A WRF-Chem study in a polluted subtropical region. J. Geophys. Res. Atmos. 121(7), 3645-3662.

Referee #2

The authors gratefully thank the reviewer for the comments and suggestions. We have revised our manuscript according to the reviewer's suggestions and comments. **All the changes and responses to the reviewers' comments are listed below point-by-point in blue according to a new line numbering in the revised manuscript. The major changes are highlighted with blue in the revised manuscript.**

The Authors have made a thorough revision of their work and addressed most of the concerns raised. Subject to some further major revisions and a thorough job of revising the manuscript for improved clarity, this work will be acceptable for publication in Atmospheric Chemistry and Physics.

Major Revisions:

1. Clarity of the manuscript is lacking. In some instances, this is due to formatting issues (e.g. reactions listed with some assigned arbitrary letters, instead of consecutive numbers), while in other instances ideas need to be separated in order to be clearly understood. In most cases, this is possible to achieve by breaking the current statements into smaller sentences. These are noted in problematic areas through the technical comments but should be revisited throughout. It is likely that this very interesting work will not receive the attention, or citations, it deserves if the clarity is not improved. The Authors should also ensure that their manuscript and reference formatting meets the journal guidelines.

Response: We thank the reviewer for the careful review, we revised the manuscript following the reviewer's major revision and technical comments. Now, the reactions have been listed with consecutive numbers, some long sentences have been broken to smaller sentences, for example: "However, the photosensitized NO_2 on humic acid could act as a source of HONO during the daytime as reported by Stemmler et al. (2006) then which might lead to a HONO morning peak within hypothesis (b)." to "As reported by Stemmler et al., (2006), the photosensitized NO_2 on humic acid could act as a source of HONO during the daytime. It was expected that the photosensitized NO_2 on humic acid might lead to a HONO morning peak within hypothesis (b)". Finally, all the co-authors went through the manuscript to correct the writing and format errors.

2. Instrument details to validate quality of the intercomparison are still lacking and need to be improved. Specifically, the following need to be addressed:

The MARGA accuracy and precision statistics for quantifying nitrite must be provided in this manuscript. Referral to when the instrument operated similarly in another study, using different solvent sources, and potentially being disassembled and reconstructed prior to use

here, does not qualify the performance it operated at in this work. Nor should the reader need to look for critical relevant details for this work in another manuscript. This is a critical revision.

Response: The MARGA system is located at the Melpitz station since 2010. For this campaign, the MARGA accuracy and precision was checked by testing the solvent blanks and by performing standard measurments when the system was set up in the field. We have added this information in the method section for the MARGA measurements in line 157-162:
"The precision for HONO quantification is below 4 % indicating a good repeatability. For the accuracy of the ion chromatography system, liquid NO_2^- standards were twice injected to the MARGA with concentrations of 70, 120 and 150 µg L^{-1}. The resulting slope of 1.13 (R^2 = 0.99) indicates slightly lower measured NO_2^- concentrations, which might be a result of nonstable NO_2^- in freshly made liquid standard solutions. Thus, a MARGA accuracy of 13% was assumed for the HONO/NO_2^- quantification."

Pages 4-5, Lines 142-150: The MARGA blanks description is still missing critical details. Were the detection limits of HONO determined for this system for this set of field observations? One detection limit determined in another work does not apply to every group using a similar instrument. It is a measure of signal to noise during the observation period.

Response: We are sorry for the misunderstanding. Exactly to determine the detection limit of the HONO measurements with the MARGA system, we performed blank measurements for the MARGA before the intercomparison campaign in 2018. We changed the sentence in line 147-156:
"The detection limits and the blanks for the MARGA system were performed before the intercomparison campaign in 2018. The detection limit of HONO was determined as 10 pptv. The blanks were analyzed when the system was set up in the field to consider potential contaminations. For blank measurements, the MARGA blank measurement mode was used that has a duration of six hours. Within the first 4 hours, the MARGA air pump was off and the denuder and SJAC liquids were analyzed. The first- and second-hour samples are discarded as they still include residual concentrations. The evaluation of the blank concentrations was performed for the third- and fourth-hour samples. No discernable peaks above the instrument detection limits were identified in both the gas and particle phase channels.

When the solvent blanks for the MARGA were analyzed, was the system set up in the field location or in the lab? If they were collected in the lab, how can the Authors rule out contamination of the solvent or instrument components as the source of the discrepancy in the subsequent intercomparison? This is not clearly stated and confounds the quality of the

intercomparison work reported.

Response: During the blank measurements, the MARGA was located at the Melpitz field site to consider potential contaminations. And we should note that the solvent blanks were analyzed when the system was set up in the field to consider potential contaminations.

Lastly, the Authors report 0.00 ug/L of nitrite in their blanks, which is misleading. The instrument has a detection limit somewhere in the neighborhood of 0.02 ug/m3, which is a non-zero value. The detection limit is derived from the instrument signal to noise, which means nitrite could be present below the detection limits in these blanks. Consider instead a statement that 'no discernable peaks above the instrument detection limits were possible to identify both in the gas and particle channels'

Response: The reviewer is right on this point. In Lines 155-156, we rewrote: "Within these blank samples, 0.00 µg l 1 of nitrite both in the gas and particle phase were measured indicating no background nitrite collection." was changed to "no discernable peaks above the instrument detection limits were identified both in the gas and particle channels"

Page 5, Lines 164-168: The LOPAP detection limit is given, but the duration of the measurement it applies to does not. Since the comparison between the MARGA and the LOPAP is only valid at the hourly timesecale, this detection limit is required. For the remainder of the data analysis in the manuscript, which uses the LOPAP observations, the detection limit that applies to the time resolution of the dataset needs to be provided – and depicted on figures where appropriate.

Response: We should note that both acidic stripping solution and 0.8 mM n-(1-naphthyl)ethylenediamine-dihydrochloride were not changed during the campaign. As we mentioned in the manuscript, calibrations were conducted on April 17th, April 20th, 24th, 25th, April 29th during the campaign. These calibrations were used to determine the detection limits for different time resolution (30 seconds and 30 minutes) and also to check the stability of LOPAP in the campaign. We added this information now in line 173-175:

"Both the acidic stripping solution and 0.8mM n-(1-naphthyl)ethylenediamine-dihydrochloride solution were kept in the dark and were not changed during the whole campaign period."

And in line 178-181:

"In addition, calibrations using NO_2^- standard solution (Heland et al., 2001) were applied in

the beginning (April 17th), middle (April 20th, 24th, 25th) and end (April 29th) of the campaign to derive the HONO mixing ratio. The detection limit of LOPAP was 0.6 pptv and 0.1 pptv for the time resolution of 30 seconds and 30 minutes, respectively…"

For the 30 seconds LOPAP data in the manuscript, the error of HONO was calculated based on the detection limit (0.6 pptv) and a relative error 10%. The error is used for our investigations in Figure 1a, Figure 2, Figure 5 and Figure 6.

The LOPAP accuracy is stated to be derived from a 'relative standard deviation' of 10 %, but how this was determined is unclear. Please clarify how this was calculated using the principles of analytical instrumentation (i.e. multiple evaluations of the calibration response, evaluation of an injected check standard). Has the propagated error from subtraction of signal in the second channel of the instrument been considered? It seems that this may not be a conservative estimate of the instrument performance and the Authors should be careful not to overstate this.

Response: The relative error is calculated by error propagation of all systematic errors, i.e. uncertainties in the gas flow ca. 2%, the liquid flow ca. 2 %, the error in the nitrite concentration during calibration 1 % +errors for the used pipettes/flasks and the 10 % is a conservative upper limit. Because all glass wares were not used exactly at 20 ℃ like recommended by the manufacturer, 2 times of the specified errors for all volumetric glass wares was applied. And finally we used a relative error of 10% in this work. We add this information in line 183-187.

"The relative error is calculated by error propagation of all systematic errors, i.e. uncertainties in the gas flow ca. 2%, the liquid flow ca. 2 %, the error in the nitrite concentration during calibration 1 % and errors for the used pipettes/flasks (two times of the specified errors of all volumetric glass ware since all glass ware was not used exactly at 20 ℃ like recommended by the manufacturer)."

Also the "real" HONO concentration is finally calculated by subtracting the value of channel 2 from channel 1, the propagated error from subtraction was also considered in the "real" HONO concentration.

Figure 1: The intercomparison regression has been performed using an orthogonal regression, yet it is unclear whether the measurement error has been included in this assessment. There are no error bars depicted on the datapoints, which suggests that appropriate regression using error-based weighting has not been applied. The lack of such consideratio could be valid if both instruments are subject to similar accuracy and precision metrics, but this information for the MARGA is not presented (see first comment in this section) makes the validity impossible to determine.

Response: We thank the reviewer for the insightful view. We added error bar for both the LOPAP data and MARGA data in Figure 1 and an orthogonal regression using error-based weighting was applied, which result the slopes of 1.57 and 1.66 for period M1 and M2, respectively. We updated this information in Figure 1 and section 3.1.

In panel (a) of the figure, it is clear that there is a major lag issue in the MARGA (i.e. the decay constant in the HONO measurement from a local maximum appears to be constant across many days, following the nocturnal maximum). The same observation is not seen in the LOPAP and also appears to be absent during M1. Clearly there is an inlet effect that is developing over time with HONO partitioning into the Teflon tubing, which would be expected if the inlet is not heated and can retain significant surface water. Further to this, particles will be depositing to the inlet material, as it is not conductive, resulting in chemical reactions between the gas flow and surface-deposited material. Both of these issues should be discussed as confounding factors in the relevant section of the manuscript.

Response: The reviewer is right with these points. It cannot be excluded that water or deposited particles have an influence on the gas- and particle phase composition by chemical reactions within the inlet. The inlet tubing of the MARGA outside of the container is surrounded by a shelter. Within the shelter, the inlet tubing is continuously ventilated with ambient air to reduce condensation or evaporation by temperature differences between sampled and air within the shelter that could favor condensation within the inlet tube.
Deviation between denuder measurements and other instruments for HONO measurements were also observed in previous studies. Volten et al., (2012) compared a miniDOAS system with an AMOR instrument for NH_3 measurements. The AMOR instrument is based on a continuous-flow wet denuder system similar to the MARGA. This group found a fast response for the miniDOAS measurements on short time scales, while the AMOR measurements showed offsets and a delay because of inlet memory effects by particles or water. Additionally, they suggest that the aqueous sample transport between sampling and analysis devices could explain a further delay. The same was described by Dammers et al., (2017), who compared a MARGA system with the miniDOAS.

These points are now discussed within the manuscript at Line 255-262: “In addition, the comparison between both instruments in Figure 1a shows a delay of the MARGA concentrations after reaching the maximum concentrations in the morning. This pattern was also observed in previous studies of Volten et al., (2012) and Dammers et al., (2017), who compared miniDOAS instruments with wet denuder systems. Compared to fast responses of the miniDOAS, the denuder-based instruments showed offsets and delays because of inlet memory artefacts by particles or water. Both groups also suggested transport effects of the

liquid samples from the sampling to the analysis unit resulting in delays and slow responses."

The Authors concluded that inlet production and denuder artefacts generating HONO from other atmospheric constituents are the source of the systematic bias observed. The argument for inlet HONO production is convincing from the results of M1 and should be possible to correct the MARGA dataset for based on tubing length and the atmospheric sample residence time, including the remaining inlet surface area upstream of the y-split fitting. However, the denuder artefacts argument is not convincing as the correlations between the two measurements are quite strong (perhaps stronger than currently depicted due to the absence of error-weighted regression). If interferences in the denuder were driving variability, they would depend on atmospheric composition that is decoupled from HONO chemistry, resulting in random error instead of systematic error. The second channel of the LOPAP should track interferences that could arise in the MARGA denuder quite well, although the magnitude would differ. The Authors could investigate the relative magnitude of the second channel signal of the LOPAP compared to the primary channel to discern the potential for additional interferences in the MARGA denuder.

Response: Kleffmann and Wiesen (2008) mentioned that most of the available intercomparison studies support that interferences are a general problem associated with chemical instruments. And the rates of interfering liquid phase reactions, i.e. PAN hydrolysis, NO_2+SO_2, NO_2+phenols, NO_2+aromatic amines (line 269-271) tend to increase with increasing pH (Kleffmann and Wiesen 2008). These chemical interferences are expected to be even more severe for instruments that collect air samples under neutral or even basic conditions (see for example, Spindler et al., 2003; Genfa et al., 2003). The MARGA system used a solution at pH=5.7 (line 132) and LOPAP used a solution at pH=0. We agree with the reviewer that the interferences in the denuder would depend on atmospheric composition, but most related to the NO_2 as expected. Figure A1 shows the plot of interference in channel 2 vs. the atmospheric NO_2 mixing ratio and which indicate a good relationship (R^2=0.778) between NO_2 and interference. In addition, since NO_2 is also the mainly precursor of atmospheric HONO (nighttime NO_2 heterogeneous conversion R2, R2a, R2b and photo enhanced NO_2 conversion R3b), which may resulting in a likely systematic error rather than random error.
In addition, we also plot the Channel 2 vs the Channel 1 of LOPAP in Figure A2 as suggested by the reviewer. A ratio of Channel 2 to the Channel 1 as 0.0078 was obtained from the linear fitting in the Figure A2. This low interference value of LOPAP compared with interference value of MARGA in denuder (58%) could due to a different wet surface in channel 2 and denuder.

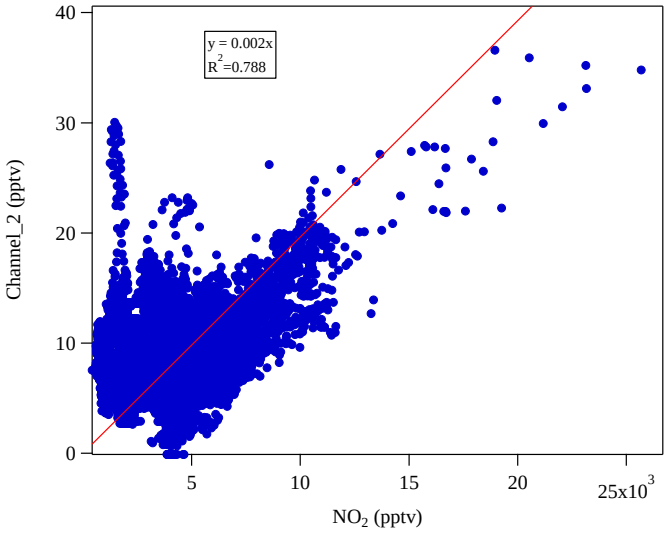

Figure A1. Plot of interference in Channel 2 of LOPAP vs the NO_2 mixing ratio in the atmosphere during the campaign period.

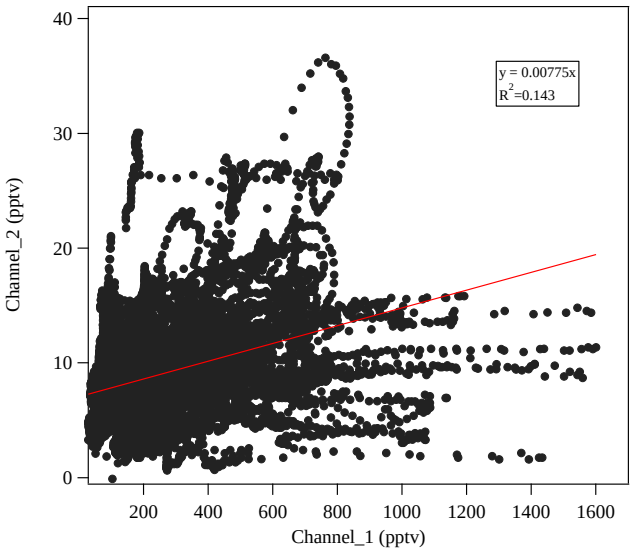

Figure A2. Plot of Channel 2 vs Channel 1 of LOPAP during the campaign period.

Finally, the ratio of MARGA to LOPAP observations from M1 are extremely close to the ratio of molecular weights between NaNO2 and the nitrite ion. The primary standard used for calibration of each instrument should be re-evaluated to ensure that these measurements are sound. There is a break in the data between M1 and M2, presumably due to instrument maintenance, as stated in the manuscript. Were both instruments recalibrated during this time? Were the same standard solutions used to calibrate both instruments? In the Reviewer's prior experience, these two considerations have been major sources of error in intercomparing instruments that rely on their calibration from aqueous nitrite standards, resulting in exactly this type of systematic error.

Response: A Titrisol (Merck) standard solution of 1000 mg of NO_2^- was used to prepare the nitrite standard solution in a 1 l volumetric flask and used to calibrate LOPAP. The same standard solution has also been used to calibrate the MARGA. The break in the data between M1 and M2 might be due to the rearrangement of LOPAP sampling unit. Additionally, the LOPAP was recalibrated after we changed the position of the LOPAP sampling unit. The MARGA setup was not changed. We should mention that the LOPAP and MARGA have been used in the groups of ICARE and TROPOS, respectively, for more than ten years and several papers have been published (Bernard et al., 2016, Laufs et al., 2017, Stieger et al., 2018).

Technical Revisions:

Page 2, Line 40: Consider denoting reactions as '(R1)' with increasing numbers for subsequent reactions. This will simplify the notation used throughout the manuscript and create greater clarity.

Response: We agree with the Reviewer, and changed e.g. "reaction 1 …" to "R1 …".

Page 2, Line 62: Should 'homogeneous nucleation' be 'homogenous reaction'?

Response: "homogeneous nucleation" was changed to "homogenous reaction" in line 62.

Page 2, Line 64: 'However' is not necessary here and is used incorrectly in many places throughout the manuscript. Its use should denote a contrasting result or statement to the preceding sentence. Similar adverbs are used where they are not required throughout the manuscript, sometimes resulting in unclear meaning of the scientific results.
Also in this sentence, the Authors should be careful to state that multiple mechanisms may contribute a significant proportion of produced HONO. The way this is currently written suggests that only one will dominate a given dataset, yet the balance of the literature is clearly demonstrating to us that there are many mechanisms at work that can vary in their importance depending on the time of day. For example, dew!

Response: We thank the Reviewer for the grammar correction and we checked all the "however" using through the manuscript. Some other adverbs like "then, therefore, when, where, since … " were also corrected. We agree with the reviewer about the statement here and hence decide to remove the sentence of "However, the dominant HONO formation mechanism is still under discussion."

Pages 2-3, Lines 66-73: The reactions presented should increase by one and be in order. The

reasoning behind denoting reactions ‘2a’ and ‘2b’ or ‘3a’ and ‘3b’ are not given and are, frankly, very distracting to keep track of given the exploration of these reactions throughout the manuscript. Further to this, there is no ‘reaction 8’ presented. Is there one that is used in the model? If not, please revise the numbering of the reactions and consider using the shorthand notation of ‘R1, R2, R3…’ throughout the manuscript.

Response: We revised the numbering of the reactions “R1, R2, R3…” throughout the manuscript as suggested by the reviewer.

Also, HA, A, and X are not defined in reaction 3b and need to be stated somewhere in the preceding manuscript.

Response: We defined “HA, A, and X” as “humic acid, activation of reductive centers and oxidants, respectively” in line 53-54.

Page 3, Line 82: This is an example where more organized reaction notation will improve clarity. ‘according to reaction 1’ can be replaced with (R1).

Response: We changed the ‘according to reaction 1’ to “(R1)” in line 82.

Pages 3-4, Lines 104-109: This addition to the manuscript is difficult to follow. The direction and magnitude of the discrepancy in the intercomparison are more important than the correlation coefficient. Which method was biased high? How can that be rationalized by considering the methodology used and the chemistry it (or the sample matrix) can promote? For example, if the denuders were always lower, there are many instances in the literature that show nitrite is oxidized to nitrate in the condensed phase in the presence of ozone. If the denuder results are systematically lower than those from the MARGA, then a chemical loss can be hypothesized. Overall, this addition to the paper needs to draw of a key result to motivate the intercomparison in this work. As it currently stands, the reasoning is not possible to follow without reading the Stieger paper in detail.

Response: We rephrased this addition: “Within the cited study HONO concentrations measured by a MARGA system and an off-line batch denuder without an inlet system were compared. Although the slope between both instruments was 1.10 with slightly higher MARGA concentrations in average, both instruments biased equally in the measured concentrations resulting in a high scattering with a coefficient of determination of $R^2 = 0.41$. The probable reason was the off-line analysis of the batch denuder sample as the resulting longer interaction of gas and liquid phase during the transport led to further heterogenous reactions. As both instruments are based on the same sampling technique, the present study

could be a good starting point for an inter-comparison between MARGA and LOPAP for HONO measurements to find possible reasons in the denuder deviations."

Page 4, Line 117: The final point of this work would be better described as 'the relative importance of dew as a sink and source of HONO'.

Response: We modified the sentence as "the relative importance of dew as a sink and source of HONO" in line 121-122.

Page 4, Line 136: Injection of 25 mL of sample onto an IC is not possible. Clarify the volume of the collected hourly samples for the MARGA and clearly describe the volume used to quantify the atmospheric analytes (e.g. 25 uL injection loop or 10 mL treated with a preconcentration column).

Response: We rephrased: "Then, the aqueous samples of the WRD (gas phase) and the SJAC (particle phase) were successively injected into two ion-chromatographs (IC) with conductivity detectors (Metrohm, Switzerland) by two syringe pumps for analyzing the anions and cations. The volume of the injection loops for the anions and cations were 250 µl and 500 µl, respectively."

Page 5, Line 170: This is confusing. Should 'settled' be another word here, such as 'selected'? This is an example of unclear writing that is present throughout the manuscript.

Response: "settled" was changed to "selected" in line 189.

Page 6, Lines 178 and 193-195: There is a concerning contradiction here on how the dew samples were analyzed. First the Authors state that they were stored for a year, which would be highly problematic as nitrite is known to be unstable in aqueous solution. Later, the Authors state that samples were analyzed within 6 hours on the MARGA. Which is it? Clarify.

Response: We are sorry for this confusion. We changed the sentence in line 196-198 to: "To evaluate the HONO emission from the dew water in the morning, the dew water was collected one year later after the HONO comparison campaign and was analyzed on May 8th, 11th, 13th and 14th 2019."

Page 6, Line 188: How do the volumes of the blanks that were collected compare to the samples? Or was the F(NO2-) from the blanks used to correct the dew water samples? Please clarify by specifically stating how these were used towards the work-up of the dew water

dataset.

Response: The volume of the blanks was approximately 50 mL since we used 2 L ultrapure water to clean the plate and gutter. We added "(~ 50 mL)" in the line 207 to mention the blank volume.
We added the NO_2^- concentration of blank in Table 2 in the first review, and note that " Final NO_2^- = Raw NO_2^- - Blank NO_2^- ".

Pages 7-8, Section 3.1: This entire section needs to be revisited in light of addressing the major revision above. The Authors use misleading statements in the current revisions, such as at Line 237 where they state their results are 'in excellent agreement' with prior findings that the MARGA instrument compares terribly with another technique. This gives the wrong impression. Consider using 'this result is consistent with' instead.

Response: We revised the section 3.1 following the Major revision. "in excellent agreement" was changed to "this result is consistent with" in line 265.

The added section on offline batch denuders here is very confusing. The relevance to the intercomparison, and evidence to back up the length of the discourse, are vague. Why is the offline batch denuder something to consider when the second channel of the LOPAP should be a direct measure of potential interfering species from the atmospheric matrix? Why does the pH matter if the Authors conclude that it was not an issue in this work? How does this relate to the systematic bias between the MARGA and LOPAP HONO measurements?

Response: We are sorry for the confusing and we decided to remove this part of discussion as it was mentioned already in the introduction.

Page 8, Lines 279-280: The daytime sample population of HONO mixing ratios is not normally distributed, the Authors should consider reporting the median values here instead of the means.

Response: The mean values were changed to "median values of 370±300 pptv and 280±210 pptv" in line 294.

Page 9, Line 311: 'led' should be 'lead'

Response: "led" was changed to "lead" in line 326.

Page 10, Line 340: Why are units in the denominator of this equation?

Response: we modified the Eq. 2 as $F_{NO2-} = \frac{[NO_2^-]\times V_{dew}}{S\times 1000}$. S is the surface area of the glass sampler as 1.5 m^2.

Page 11, Line 381: Should be 'least squares regression'

Response: "least linear regression" was changed to "least squares regression" in line 396.

Page 11, Lines 384-385: Give the ratio or the percentage only. No need for both.

Response: The percentage was deleted.

Page 12, Lines 397-399: The added statement is too speculative on a single specific mechanism. Consider stepping back from a single mechanism to explain the differences and instead emphasize the increasing need for more diverse environmental observations to understand HONO production chemistry in the nocturnal atmosphere.

Response: The statement of "This could be ascribed to the higher S/V surface in the rural site because of the high leaf area index (LAI, m^2/m^2) compared to an urban and might have enhanced the heterogeneous NO_2-HONO conversion." was changed to "The higher value may suggest that a more efficient heterogeneous conversion from NO_2 to HONO is present in rural sites than in urban sites." In line 413-414.

Page 12, Line 405: This equation should be inserted as all the other equations in the manuscript have been. All equation numbers through the manuscript will need to be revised following this.

Response: "$f(RH)=1+a\times(RH/100)^b$" was named as Eq. 3 in line 422.

Page 12, Lines 412-421: This section is a contradiction of itself between the first sentence and the last. First the Authors state that all the HONO could be produced on the aerosol, using reactive uptake coefficients consistent with the literature from lab studies, but inconsistent with observations of the full nocturnal boundary layer profiles of HONO and its precursors. The Authors then state that the correlation between [HONO]/[NO2] versus Sa is sufficient evidence that this mechanism is not important, yet the correlation is moderate in magnitude. This is a weak argument that needs to be reworked. The Authors are encouraged to visit the recent work from the group of Jochen Stutz to better place their findings and reasoning regarding aerosol-mediated NO2-to-HONO conversion into the context of our current

understanding.

Response: In this section, we firstly assume all the HONO could be formed on the aerosol, then an uptake coefficient of NO_2 on the aerosol surface $\gamma_{NO2\rightarrow HONO\_a}$ as 2.8×10^{-5} - 3.8×10^{-4} was obtained in this work. We corrected this value from previous version since we made a mistake for the Sa ($dN/d\log D_\rho$ was wrongly used from size distribution, here we correctly use a real particle number N). And this theoretical uptake coefficient falls into a reasonable range (10^{-6} - 10^{-4}) similar to former studies which normally is regarded as unimportant for the HONO formation through heterogeneous NO_2 conversion on particle surfaces. This conclusion was also confirmed from a weak correlation between HONOcorr/NO_2 vs Sa. We modified this part as "Assuming the entire HONO formation was taking place on the particle surface, the calculated $\gamma_{NO2\rightarrow HONO\_a}$ from the Eq. 4 varied from 2.8×10^{-5} to 3.8×10^{-4} with a mean value of $(1.7\pm1.0)\times10^{-4}$. This theoretical uptake coefficient falls into a reasonable range of 10^{-6} - 10^{-4} similar to former studies (Kleffmann et al., 1998, Kurtenbach et al., 2001, Wong et al., 2011, VandenBoer et al., 2013). However, considering the weak correlation between $HONO_{corr}$ (R^2=0.566), $HONO_{corr}$/ NO_2 (R^2=0.208) and S_a (Figure S6), the relative amount of HONO formed on particle surfaces might be small as previously reported (Kalberer et al., 1999, Sörgel et al., 2011, Wong et al., 2011)." in line 429-437.

Page 14, Lines 484-493: The Authors need to be careful here with their reasoning. Bulk water pH collected from a glass surface into a bottle does not directly translate into bulk water pH for dew found on soil or vegetated surfaces. The chemical nature of the material, with which the water is in contact, can influence the effective pH. A cautionary statement should be made here.

Response: We add a cautionary statement as "However, it should be noted that the measured pH of collected dew from the glass plate might differ compared to the pH of dew found on soil or vegetated surfaces. The chemical nature of the material, with which the water is in contact, can influence the effective pH." In line 511-514.

At Line 490 there are too many significant digits. Correct this.

Response: We changed the number as "42 and 165 mg L^{-1}" in line 507.

Page 16, Line 531: Clarity can be improved. Consider 'used are' instead of 'are referred to'

Response: "are referred to" was changed to "used are" in line 547.

Page 16, Line 542: Clarity can be improved. Consider 'expect that the reaction between NO

and OH' instead of 'indicate that the reaction 3a'.

Response: We changed "expect that the reaction between NO and OH" instead of "indicate that the reaction R7". R7 is a new number of previous reaction 3a.

Page 16, Line 544-546: This sentence is unclear. Rephrase.

Response: We rephrased the sentence as "However, regarding on the large uncertainty of [OH] (a factor of 2), the "unknown HONO sources" exist but could be not crucial" in line 560-561.

Page 19, Line 630: Why is mixing height spelled out here instead of using the variable 'H' in this equation?

Response: We corrected our Eq. 17 as:

$$[HONO] = \frac{\alpha \times S_g \times F_{NO2-}}{H \times S_g} = \frac{\alpha \times F_{NO2-}}{H} \quad \text{(Eq. 17)}$$

F_{NO2^-} is the NO_2^- concentration per m^2 of the glass sampler surface. The mean F_{NO2^-} from May 11th 2019 was used for the calculation. S_g represents the surface area of the flat ground (analog to the surface area of the glass sampler), α is the enhanced factor for V_{dew} (dew water sample volume of the glass sampler in Eq.2) due to the larger cold surfaces from grass which can get in contact with humid air than the flat glass sampler. α was calculated as 2×LAI to take the areas on both sides of the leaves and the vegetation-covered areas on the ground into account. Regarding the grass height during the dew measurements (~30cm) that is approximately the height in April 2018 and May 2019, we used a factor of 6 for LAI.

Page 20, Lines 664-665: Reference formatting is incorrect. Ensure this is to journal guidelines throughout the manuscript prior to resubmission.

Response: We corrected and checked all the reference format of manuscript.

Page 30, Table 2: The nitrite detection limits for the MARGA in terms of concentration need to be considered. Some of the entries here are very small and may be below the instrument detection limits. In such cases, appropriate notation should be given for this and the detection limit given in the footnotes.

Response: We added the notation "[a] note that the blank NO_2^- concentration is lower than the detection limit of MARGA 0.0.02 μg L^{-1}." for Table 2. The detection limit is 0.0.02 μg L^{-1}. Please add as footnote!

Page 35, Figure 3: The scales for the different axes overlap on the left and right sides of the figure and space between them should be added. The particulate nitrite measurements look like they are often below the detection limit and either the LOD needs to be depicted on that figure or those points should have different symbols/be excluded. Why is the presence of PM10 nitrite not discussed in the manuscript, particularly for the intercomparison? Could deposition of this PM10 nitrite in the inlet lines or denuder contribute to the systematic difference between the MARGA and LOPAP observations?

Response: The Figure 3 was improved as suggested by the reviewer.
A Steam-Jet Aerosol Collector (SJAC) is used in the MARGA system, which uses 100 ℃ hot water steam forming droplets. On the droplets, different reactions of NO_2 can form nitrite as a function of temperature (e.g. NO_2 + organics, Gutzwiller et al.). Thus, we used our aerosol nitrite MARGA data with caution and present them in Figure 3. In addition, Figure 3 shows that particulate NO_2^- is mainly observed during high HONO concentrations indicating a HONO breakthrough towards the SJAC. Assuming that measured NO_2^- is measured HONO within the SJAC, the ratio between measured NO_2^- and HONO concentrations was 1.8 % in the present study. This is low compared with systematic difference between the MARGA and LOPAP observations. A sum of WRD and SJAC NO_2^- concentrations would further increase the MARGA HONO concentration leading stronger deviations. Because of likely interferences, we decided to remove the NO_2^- values from Figure 3.

Page 38, Figure 6: The note on the reactions should be removed from the caption after re-assigning appropriate reaction numbers throughout the manuscript. Then R1, R3, or R9 in the figure legend are easily cross-referenced and several lines of caption are no longer necessary.

Response: The notes on the reactions have been removed from the caption and we also improved the Figure legend.

The figure and associated legend are too complicated and can be easily simplified The Authors state in the discussion that their base case is Model 3, and therefore, should not depict Models 1 or 2 on this figure. The composition of 'Model 3' should be given in the caption and then only the additional terms would need to be stated for the subsequent model runs. The runs, as they currently are described, are confusing.

Response: In the discussion part, we mention that Model 1 and Model 2 are used to discuss the HONO contribution from the gas-phase reaction of NO with OH radical and HONO deposition on the ground surface independent on RH, respectively. The base case for Model 4, 5 and 6 is Model 3. Hence, we kept all the Models (1, 2, 3, 4, 5 and 6) in the Figure and

simplified the legend by note them in the caption as "Pss presents model results by assuming an instantaneous photo-equilibrium between the gas-phase formation (R7) and gas-phase loss processes (R1 and R11) of HONO; Model 1 includes R1+R7+R11. Model 2 includes R1+R2+R7+R11+surface deposition (00:00-00:00), whereas Model 3 describes R1+R2+R7+R11+surface deposition (17:00-8:00). And Model 3 is used to be the base to investigate the effect of R9 (Model 4), R5 (Model 5) and the combination of R5+R9+Dew HONO emission (4:30-7:00) (Model 6).".

Panel a from this figure is not necessary. It can either be removed entirely or relocated to the SI.

Response: We removed the Panel a.

Page 39, Figure 7: The terms on the axis labels for this figure are confusing and should be revised. It is not clear why 'internal time' is necessary to retain, when UTC can be used to better effect.

Response: As we can see in Figure 7 and also Figure 2, the time of HONO morning peak was little different with each day. Hence we defined the relationship between temporary HONO emission from dew water and decreasing RH with internal time not UTC in Eq. 15. Here we improved the Figure 7 by moving UTC to the bottom.

Supporting Information, Page 2, Figure S1: The three photos should be denoted as panels a, b, and c. The inlet photo should be panel a, followed by the M1 setup in panel b, and then the M2 setup in panel c. Delete the 'Figure S1a' and 'Figure S1b' from below the photos.

Response: We improved the Figure S1 following the reviewer's suggestion.

Supporting Information, Page 5, Figure S4: Fix axis overlap to improve clarity.

Response: We improved the Figure S4.

Supporting Information, Page 9, Figure S8: What range of dates does the depicted data originate from?

Response: We mentioned the dates "during the campaign period (April 19th to 29th, 2018)" in the caption.

Supporting Information, Page 12, Figure S10: This figure is very confusing to follow, mostly

due to the presentation of panel b. Why is it noted before panel a? Why is RH on the horizontal axis? Fix this. Place the panel b to the right panel a, and depict HONO_unknown increasing as a function of RH if anything. Since this plot includes all the different days of the observations, it is very hard to see the utility of it. Presumably, this is to show that rapid humidity changes result in the release of HONO. Either a case study showing this from a single day should be given, or a more robust analysis performed to demonstrate this phenomenon.

Response: We improved the Figure S10 as suggested by the reviewer.

Supporting Information, Page 13, Figure S11: Delete the 'Note' since the reaction notation throughout the manuscript should be fixed anyways, making this no longer necessary.

Response: We deleted the note and also modified the legend.

Reference

Acker, K. and Möller, D., 2007. Corrigendum to: Atmospheric variation of nitrous acid at different sites in Europe. Environ. Chem. 4(5), 364-364.

Alicke, B., Geyer, A., Hofzumahaus, A., Holland, F., Konrad, S., Pätz, H.W., Schäfer, J., Stutz, J., Volz-Thomas, A. and Platt, U., 2003. OH formation by HONO photolysis during the BERLIOZ experiment. J. Geophys. Res. Atmos. 108(D4), 8247.

Alicke, B., Platt, U. and Stutz, J., 2002. Impact of nitrous acid photolysis on the total hydroxyl radical budget during the Limitation of Oxidant Production/Pianura Padana Produzione di Ozono study in Milan. J. Geophys. Res. Atmos. 107(D22), 8196.

Bernard, F., Cazaunau, M., Grosselin, B., Zhou, B., Zheng, J., Liang, P., Zhang, Y.J., Ye, X.N., Daële, V., Mu, Y.J., Zhang, R.Y., Chen, J.M. and Mellouki, A., 2016. Measurements of nitrous acid (HONO) in urban area of Shanghai, China. Environmental Science and Pollution Research 23(6), 5818-5829.

Cai, R., Yang, D., Fu, Y., Wang, X., Li, X., Ma, Y., Hao, J., Zheng, J. and Jiang, J., 2017. Aerosol surface area concentration: a governing factor in new particle formation in Beijing. Atmos. Chem. Phys. 17(20), 12327-12340.

Dammers, E., Schaap, M., Haaima, M., Palm, M., Kruit, R.J.W., Volten, H., Hensen, A., Swart, D. and Erisman, J.W., 2017. Measuring atmospheric ammonia with remote sensing campaign: Part 1-Characterisation of vertical ammonia concentration profile in the centre of The Netherlands. Atmos. Environ. 169, 97-112.

del Campo, A.D., Navarro, R.M., Aguilella, A. and González, E., 2006. Effect of tree shelter design on water condensation and run-off and its potential benefit for reforestation establishment in semiarid climates. For. Ecol. Manag. 235(1), 107-115.

Guan, H., Sebben, M. and Bennett, J., 2014. Radiative- and artificial-cooling enhanced dew collection in a coastal area of South Australia. Urban Water Journal 11(3), 175-184.

Heland, J., Kleffmann, J., Kurtenbach, R. and Wiesen, P., 2001. A New Instrument To Measure Gaseous Nitrous Acid (HONO) in the Atmosphere. Environ. Sci. Technol. 35(15), 3207-3212.

Kalberer, M., Ammann, M., Arens, F., Gäggeler, H.W. and Baltensperger, U., 1999. Heterogeneous formation of nitrous acid (HONO) on soot aerosol particles. J. Geophys. Res. Atmos. 104(D11), 13825-13832.

Kleffmann, J., Becker, K.H. and Wiesen, P., 1998. Heterogeneous NO_2 conversion processes on acid surfaces: Possible atmospheric implications. Atmos. Environ. 32(16), 2721-2729.

Kleffmann, J. and Wiesen, P., 2008. Technical Note: Quantification of interferences of wet chemical HONO LOPAP measurements under simulated polar conditions. Atmos. Chem. Phys. 8(22), 6813-6822.

Kotzen, B., 2015. Innovation and evolution of forms and materials for maximising dew collection. Ecocycles 1(1), 39-50.

Kurtenbach, R., Becker, K.H., Gomes, J.A.G., Kleffmann, J., Lörzer, J.C., Spittler, M., Wiesen, P., Ackermann, R., Geyer, A. and Platt, U., 2001. Investigations of emissions and heterogeneous formation of HONO in a road traffic tunnel. Atmos. Environ. 35(20), 3385-3394.

Laufs, S., Cazaunau, M., Stella, P., Kurtenbach, R., Cellier, P., Mellouki, A., Loubet, B. and Kleffmann, J., 2017. Diurnal fluxes of HONO above a crop rotation. Atmos. Chem. Phys.

17(11), 6907-6923.
Li, D., Xue, L., Wen, L., Wang, X., Chen, T., Mellouki, A., Chen, J. and Wang, W., 2018. Characteristics and sources of nitrous acid in an urban atmosphere of northern China: Results from 1-yr continuous observations. Atmos. Environ. 182, 296-306.
Li, X., Brauers, T., Häseler, R., Bohn, B., Fuchs, H., Hofzumahaus, A., Holland, F., Lou, S., Lu, K.D., Rohrer, F., Hu, M., Zeng, L.M., Zhang, Y.H., Garland, R.M., Su, H., Nowak, A., Wiedensohler, A., Takegawa, N., Shao, M. and Wahner, A., 2012. Exploring the atmospheric chemistry of nitrous acid (HONO) at a rural site in Southern China. Atmos. Chem. Phys. 12(3), 1497-1513.
Liu, Z., Wang, Y., Costabile, F., Amoroso, A., Zhao, C., Huey, L.G., Stickel, R., Liao, J. and Zhu, T., 2014. Evidence of Aerosols as a Media for Rapid Daytime HONO Production over China. Environmental Science & Technology 48(24), 14386-14391.
Sörgel, M., Regelin, E., Bozem, H., Diesch, J.-M., Drewnick, F., Fischer, H., Harder, H., Held, A., Hosaynali-Beygi, Z., Martinez, M. and Zetzsch, C., 2011. Quantification of the unknown HONO daytime source and its relation to NO_2. Atmos. Chem. Phys. 11(20), 10433-10447.
Stemmler, K., Ammann, M., Donders, C., Kleffmann, J. and George, C., 2006. Photosensitized reduction of nitrogen dioxide on humic acid as a source of nitrous acid. Nature 440, 195.
Stieger, B., Spindler, G., Fahlbusch, B., Müller, K., Grüner, A., Poulain, L., Thöni, L., Seitler, E., Wallasch, M. and Herrmann, H., 2018. Measurements of PM_{10} ions and trace gases with the online system MARGA at the research station Melpitz in Germany – A five-year study. J. Atmos. Chem. 75(1), 33-70.
VandenBoer, T.C., Brown, S.S., Murphy, J.G., Keene, W.C., Young, C.J., Pszenny, A.A.P., Kim, S., Warneke, C., de Gouw, J.A., Maben, J.R., Wagner, N.L., Riedel, T.P., Thornton, J.A., Wolfe, D.E., Dubé, W.P., Öztürk, F., Brock, C.A., Grossberg, N., Lefer, B., Lerner, B., Middlebrook, A.M. and Roberts, J.M., 2013. Understanding the role of the ground surface in HONO vertical structure: High resolution vertical profiles during NACHTT-11. J. Geophys. Res. Atmos. 118(17), 10,155-110,171.
Volten, H., Bergwerff, J.B., Haaima, M., Lolkema, D.E., Berkhout, A.J.C., van der Hoff, G.R., Potma, C.J.M., Kruit, R.J.W., van Pul, W.A.J. and Swart, D.P.J., 2012. Two instruments based on differential optical absorption spectroscopy (DOAS) to measure accurate ammonia concentrations in the atmosphere. Atmos. Meas. Tech. 5(2), 413-427.
Wang, G., Zhang, R., Gomez, M.E., Yang, L., Levy Zamora, M., Hu, M., Lin, Y., Peng, J., Guo, S., Meng, J., Li, J., Cheng, C., Hu, T., Ren, Y., Wang, Y., Gao, J., Cao, J., An, Z., Zhou, W., Li, G., Wang, J., Tian, P., Marrero-Ortiz, W., Secrest, J., Du, Z., Zheng, J., Shang, D., Zeng, L., Shao, M., Wang, W., Huang, Y., Wang, Y., Zhu, Y., Li, Y., Hu, J., Pan, B., Cai, L., Cheng, Y., Ji, Y., Zhang, F., Rosenfeld, D., Liss, P.S., Duce, R.A., Kolb, C.E. and Molina, M.J., 2016. Persistent sulfate formation from London Fog to Chinese haze. Proceedings of the National Academy of Sciences 113(48), 13630-13635.
Wang, J., Zhang, X., Guo, J., Wang, Z. and Zhang, M., 2017. Observation of nitrous acid (HONO) in Beijing, China: Seasonal variation, nocturnal formation and daytime budget. Sci. Total Environ. 587, 350-359.
Wentworth, G.R., Murphy, J.G., Benedict, K.B., Bangs, E.J. and Collett Jr., J.L., 2016. The role of dew as a night-time reservoir and morning source for atmospheric ammonia. Atmos.

Chem. Phys. 16(11), 7435-7449.
Wong, K.W., Oh, H.-J., Lefer, B.L., Rappenglück, B. and Stutz, J., 2011. Vertical profiles of nitrous acid in the nocturnal urban atmosphere of Houston, TX. Atmos. Chem. Phys. 11(8), 3595-3609.
Zhang, L., Wang, T., Zhang, Q., Zheng, J., Xu, Z. and Lv, M., 2016. Potential sources of nitrous acid (HONO) and their impacts on ozone: A WRF-Chem study in a polluted subtropical region. J. Geophys. Res. Atmos. 121(7), 3645-3662.

Role of the dew water on the ground surface in HONO distribution: a case measurement in Melpitz

Yangang Ren[1], Bastian Stieger[2], Gerald Spindler[2], Benoit Grosselin[1], Abdelwahid Mellouki[1*], Thomas Tuch[2], Alfred Wiedensohler[2], Hartmut Herrmann[2*],

1. Institut de Combustion, Aérothermique, Réactivité et Environnement (ICARE), CNRS (UPR 3021), Observatoire des Sciences de l'Univers en région Centre (OSUC), 1C Avenue de la Recherche Scientifique, 45071 Orléans Cedex 2, France

2. Leibniz Institute for Tropospheric Research (TROPOS), Permoserstraße 15, 04318 Leipzig, Germany

***** Corresponding author: Abdelwahid Mellouki (abdelwahid.mellouki@cnrs-orleans.fr) and Hartmut Herrmann (herrmann@tropos.de)

Abstract: To characterize the role of dew water for the ground/surface HONO distribution, nitrous acid (HONO) measurements with a MARGA and a LOPAP instrument were performed at the TROPOS research site in Melpitz from April 19th to 29th, 2018. The dew water was also collected and analyzed from May 8th to 14th, 2019 using a glass sampler. The high time resolution of HONO measurements showed characteristic diurnal variations that revealed: (i) vehicle emission is a minor source of HONO at the Melpitz station; (ii) heterogeneous conversion of NO_2 to HONO on ground surface dominates HONO production at night; (iii) there is significant nighttime loss of HONO with a sink strength of 0.16±0.12 ppbv h^{-1}; (iv) dew water with mean NO_2^- of 7.91±2.14 μg m^{-2} could serve as a temporary HONO source in the morning when the dew droplets evaporate. The nocturnal observations of HONO and NO_2 allowed direct evaluation of the ground uptake coefficients for these species at night: $\gamma_{NO2\rightarrow HONO} = 2.4\times10^{-7}$ to 3.5×10^{-6}, $\gamma_{HONO,ground} = 1.7\times10^{-5}$ to 2.8×10^{-4}. A chemical model demonstrated that HONO deposition to the ground surface at night was 90-100% of the calculated unknown HONO source in the morning. These results suggest that dew water on the ground surface was controlling the temporal HONO distribution rather than straightforward NO_2–HONO conversion. This can strongly enhance the OH reactivity throughout morning time or other planted areas that provide large amount of ground surface based on the OH production rate calculation.

Keywords: HONO, ground surface, NO_2–HONO conversion, dew water, OH production

1 Introduction

Nitrous acid (HONO) is important in atmospheric chemistry as its photolysis (R1) is an important source of OH radicals. In the troposphere, OH radicals can initiate daytime photochemistry, not at least leading to the formation of ozone (O_3) and secondary organic aerosol (SOA).

$$HONO + h\nu \rightarrow OH + NO \quad (R1)$$

At present, the mechanisms of HONO formation have been and are still widely discussed. In the absence of light, heterogeneous reactions of NO_2 occur on wet surfaces (R2) and are considered to be an important source of HONO according to both laboratory studies and field observations (Acker et al., 2004).

$$2NO_2 + H_2O \rightarrow HONO + HNO_3 \quad (R2)$$

Finlayson-Pitts et al. (2003) proposed a mechanism (R3) involving the formation of the NO_2 dimer (N_2O_4) especially during nighttime. However, this pathway is not important in the real atmosphere (Gustafsson et al., 2008). The surface of soot (Ammann et al., 1998;Arens et al., 2001;Gerecke et al., 1998) or light activated soot (Aubin and Abbatt, 2007;Monge et al., 2010) contain functionalities attached to the large carbonaceous structures or individual condensed organic species, like phenol (R4) (Gutzwiller et al., 2002) and light-activated humic acids (Stemmler et al., 2006), which undergo electron transfer reactions with NO_2 yielding HONO (R5, where HA, A^{red}, and X are humic acid, activation of reductive centers and oxidants, respectively). This reaction is also postulated for aromatics in the aqueous phase, but only proceeds at a relevant rate at high pH levels (Ammann et al., 2005;Lahoutifard et al., 2002). Gustafsson et al. (2008) provide the evidence that formation of HONO proceeds by a bimolecular reaction of absorbed NO_2 and H (R6) on mineral dust, where H formed from the dissociation of chemisorbed water. However, Finlayson-Pitts (2009) indicated that this pathway is probably not transferable from laboratory to real atmosphere. In addition to the direct emission from the vehicle exhaust (Kurtenbach et al., 2001) and homogeneous gas phase reaction of NO with OH (R7) (Pagsberg et al., 1997), some other HONO formation mechanisms have been proposed e.g. homogeneous reaction of NO_2, H_2O, and NH_3 (R8) (Zhang and Tao, 2010); photolysis of nitric acid and nitrate (HNO_3/NO_3^-) (R9) (Ye et al., 2016;Zhou et al., 2011) and nitrite emission from soil (R10) (Su et al., 2011).

$$2NO_2\,(g) \leftrightarrow N_2O_4\,(g) \leftrightarrow N_2O_4\,(surface) \leftrightarrow HONO\,(surface) + HNO_3\,(surface) \quad (R3)$$

$$NO_2 + \{C\text{–}H\}_{red} \rightarrow HONO + \{C\}_{ox} \quad (R4)$$

$$HA \xrightarrow{h\nu} A^{red} + X;\ A^{red} + X \rightarrow A';\ A^{red} + NO_2 \rightarrow A'' + HONO \quad (R5)$$

$$NO_2\,(ads) + H\,(ads) \rightarrow HONO\,(ads) \rightarrow HONO\,(g) \quad (R6)$$

$$NO + OH \rightarrow HONO \quad (R7)$$

$$NO_2\,(g) + H_2O\,(g) + NH_3\,(g) \rightarrow HONO\,(g) + NH_4NO_3\,(s) \quad (R8)$$

$HNO_3/NO_3^- + h\nu \rightarrow HONO/NO_2^- + O$ (R9)

NO_2^- (aq) + H+ (aq) → HONO (aq) (R10)

Several studies (Acker et al., 2004;He et al., 2006;Lammel and Perner, 1988;Lammel and Cape, 1996;Rubio et al., 2009;VandenBoer et al., 2013;VandenBoer et al., 2014) reported that deposited HONO on wet surfaces can be a source for observed daytime HONO. Few of them have simultaneously quantified both dew and atmospheric composition. He et al. (2006) observed HONO released from a drying forest canopy and their lab studies showed that, on average, ~90% of NO_2^- was emitted as HONO during dew evaporation. Rubio et al. (2009) found a positive correlation between formaldehyde and HONO in dew and the atmosphere.

The dominant loss of HONO is photolysis during daytime, which forms OH radicals (R1). An additional sink of HONO is the reaction with OH radical (R11). Due to the absence of solar radiation and the low OH concentration, the main loss process of HONO during nighttime is dry deposition, which can reach the balance with HONO production and vertical mixing to generate a steady state of HONO mixing ratio.

$HONO + OH \rightarrow H_2O + NO_2$ (R11)

Due to its significant atmospheric importance, HONO has been measured for many years with various techniques (Febo et al., 1993;Huang et al., 2002;Kanda and Taira, 1990;Platt et al., 1980;Schiller et al., 2001;Wang and Zhang, 2000). LOng Path Absorption Photometer (LOPAP) is a two channel in situ HONO measurement instrument, which detects HONO continuously by wet sampling and photometric detection. LOPAP is very selective without sampling artefact and chemical interferences (e.g. NO_2, NO, O_3, HCHO, HNO_3, SO_2 and PAN etc.). In addition, the detection limit of LOPAP can go down to 0.2 pptv (Kleffmann and Wiesen, 2008) by optimizing the parameters like (a) sample gas flow rate, (b) liquid flow rates, and (c) the length of the absorption tubing (Heland et al., 2001). LOPAP was validated and compared with the most established and reliable HONO instrument Differential Optical Absorption Spectroscopy (DOAS) Both were used in the field and in a large simulation chamber under various conditions resulting in excellent agreement (Heland et al., 2001;Kleffmann et al., 2006).

The Monitor for AeRosols and Gases in ambient Air (MARGA) is a commercial instrument combining a Steam-Jet Aerosol Collector (SJAC) and a Wet Rotating Denuder (WRD), which can quantify the inorganic water-soluble PM ions (Cl^-, NO_3^-, SO_4^{2-}, NH_4^+, Na^+, K^+, Mg^{2+}, Ca^{2+}) and corresponding trace gases (HCl, HONO, HNO_3, SO_2, NH_3). In recent years, MARGA measurements were performed worldwide, which has been summarized by Stieger et al. (2018). Within the cited study HONO concentrations measured by a MARGA system and an off-line batch denuder without an inlet system were compared. Although the slope between both instruments was 1.10 with slightly higher MARGA concentrations in average, both instruments biased equally in the measured concentrations resulting in a high

scattering with a coefficient of determination of $R^2 = 0.41$. The probable reason was the off-line analysis of the batch denuder sample as the resulting longer interaction of gas and liquid phase during the transport led to further heterogenous reactions. As both instruments are based on the same sampling technique, the present study could be a good starting point for an inter-comparison between MARGA and LOPAP for HONO measurements to find possible reasons in the denuder deviations.

In this study, we present parallel measurements of HONO using LOPAP and MARGA in Melpitz, Germany, over two weeks in 2018. For further investigations, dew water was collected and analyzed from May 8th to 14th 2019 using two glass samplers. In addition, other water-soluble compounds, such as gaseous HNO_3, NH_3 and particulate NO_3^-, SO_4^{2-}, NH_4^+, Na^+, K^+, Mg^{2+}, Ca^{2+}, trace gases (NO_x, SO_2 and O_3) and meteorological parameters were also measured simultaneously. Our observations provide a direct inter-comparison between LOPAP and MARGA for HONO field measurement, additional insights into HONO chemical formation processes and examine the relative importance of dew as a sink and source of HONO.

2 Experimental

2.1 Site description

Measurements were performed at the research station of the Leibniz Institute for Tropospheric Research (TROPOS) in Melpitz (12°56′E, 51°32′N). This rural field site is situated on a meadow and surrounded by flat grass land, agricultural areas and forests. The Melpitz site mainly can be influenced by two different wind direction: west wind origin from the marine crossing a large area of Western Europe and the city of Leipzig (41 km NE), and east wind crossing Eastern Europe (Spindler et al., 2004).

2.2 MARGA instrument

The MARGA (1S ADI 2080, The Netherlands) used in this study has already been described in Stieger et al. (2018). Hence, only short information is provided here. An inlet flow of 1 m^3 hr^{-1} was drawn into the sampling box after passing through an inside Teflon-coated PM_{10} inlet (URG, Chapel Hill, 3.5 m). Within the sample box, the sampled air laminarly passed a WRD, in which water-soluble gases diffuse into a 10 mg l^{-1} hydrogen peroxide (H_2O_2) solution at pH = 5.7. Particles can reach the SJAC because of their smaller diffusion velocities. Within the SJAC, the particles grow into droplets under supersaturated water vapor conditions and were collected by a cyclone. The gas and particle samples are both collected over the course of one hour. Then, the aqueous samples of the WRD (gas phase) and the SJAC (particle phase) were successively injected into two ion-chromatographs (IC) with conductivity detectors (Metrohm, Switzerland) by two syringe pumps for analyzing the anions and cations. The

volume of the injection loops for the anions and cations were 250 µl and 500 µl, respectively. The Metrosep A Supp 10 (75/4.0) column and Metrosep C4 (100/4.0) column were used to separate anions and cations, respectively. Lithium bromide was used as the internal standard for both gas- and particle-phase samples added during the sample injection to the IC.

The detection limits and the blanks for the MARGA system were performed before the intercomparison campaign in 2018. The detection limit of HONO was determined as 10 pptv. The blanks were analyzed when the system was set up in the field to consider potential contaminations. For blank measurements, the MARGA blank measurement mode was used that has a duration of six hours. Within the first 4 hours, the MARGA air pump was off and the denuder and SJAC liquids were analyzed. The first- and second-hour samples are discarded as they still include residual concentrations. The evaluation of the blank concentrations was performed for the third- and fourth-hour samples. No discernable peaks above the instrument detection limits were identified in both the gas and particle phase channels.

The precision for HONO quantification is below 4 % indicating a good repeatability. For the accuracy of the ion chromatography system, liquid NO_2^- standards were twice injected to the MARGA with concentrations of 70, 120 and 150 µg L^{-1}. The resulting slope of 1.13 (R^2 = 0.99) indicates slightly lower measured NO_2^- concentrations, which might be a result of nonstable NO_2^- in freshly made liquid standard solutions. Thus, a MARGA accuracy of 13% was assumed for the HONO/NO_2^- quantification.

2.3 LOPAP instrument

The LOPAP (QUMA, Germany) employed in this work was described in previous studies (Bernard et al., 2016;Heland et al., 2001). Only brief description is given here. The LOPAP instrument consists of two sections: a sampling unit and a detection unit. The ambient air was sampled in the sampling unit, which composed of two glass coils in series where the first coil (channel 1) accounted for HONO with interferences and the second coil (channel 2) sampled only interferences assuming that more than 99 % of HONO was absorbed into acidic stripping solution (pH=0) to form diazonium salt in channel 1. This salt reacts with a 0.8mM n-(1-naphthyl)ethylenediamine-dihydrochloride solution to produce final azo dye, which is photometrically detected by long path absorption in a special Teflon tubing (Heland et al., 2001;Kleffmann et al., 2006). During our field campaign in Melpitz, both the acidic stripping solution and 0.8mM n-(1-naphthyl)ethylenediamine-dihydrochloride solution were kept in the dark and were not changed during the whole campaign period. The temperature of the stripping coil was kept constant at 25 ℃ by a thermostat. Automatic zero air (Air liquid, Alphagaz 2, 99.9999%) measurements were performed for 30 min per 12 h measurements to correct for zero drifts. In addition, calibrations using NO_2^- standard solution (Heland et al., 2001) were applied in the beginning (April 17th), middle (April 20th, 24th, 25th) and end (April

29th) of the campaign to derive the HONO mixing ratio. The detection limit of LOPAP was 0.6 pptv and 0.1 pptv for the time resolution of 30 seconds and 30 minutes, respectively. The error of HONO mixing ratio was estimated based on these detection limits and a relative error of 10%. The relative error is calculated by error propagation of all systematic errors, i.e. uncertainties in the gas flow ca. 2%, the liquid flow ca. 2 %, the error in the nitrite concentration during calibration 1 % and errors for the used pipettes/flasks (two times of the specified errors of all volumetric glass ware since all glass ware was not used exactly at 20 ℃ like recommended by the manufacturer).

To investigate the possible sampling inlet and denuder artefacts of the MARGA, two different positions were selected for LOPAP during the measurement period (explained in SI): (M1) sampling unit of LOPAP was connected to the MARGA inlet in the back of the 2 m sampling tube and the PM_{10} inlet of MARGA as shown in Figure S1a (April 18th, 2018 13:00 UTC –April 20th, 2018 08:00 UTC); (M2) the sampling unit of LOPAP was settled in the same level as the sampling head of MARGA (Figure S1b) (April 20th, 2018 15:00 UTC –April 29th, 2018 07:00 UTC).

2.4 Dew water collection and analysis

To evaluate the HONO emission from the dew water in the morning, the dew water was collected one year later after the HONO comparison campaign and was analyzed on May 8th, 11th, 13th and 14th 2019. Similar conditions (grass height, dew formation and day length) were observed to improve the evaluation. For dew sampling, a glass sampler was used (as shown in Figure S2). Two 1.5 m^2 glass plates (Plate 1 and Plate 2) were placed 40 cm above the ground with a tilt angle of approximately 10 °. A gutter was installed at the lower end of each plates to collect the running down water. The water is trapped in 500 ml bottles. The dew samplers were prepared each evening before a likely dew event occurred (low dew point difference, clear sky and low winds). Each plate was rinsed with at least 2 L ultrapure water. A squeegee removed the excess water. Afterwards, the plates were cleaned with ethanol and were again rinsed by 2 L ultrapure water. The plate was splashed with ultrapure water and squeegeed six times and the gutter was cleaned. The sample of the sixth splash was collected as blank (~ 50 mL).

The dew water normally was collected from 18:00 to 5:00 (UTC). In the morning, the excess dew on the plate was squeegeed. To achieve the volume of dew (V_{dew}), the bottles were weighted before and after sampling by a balance. The pH was measured by a pH meter (mod. Lab 850, Schott Instruments) on a subsample of the total volume. After sampling, the aqueous solutions were filtered and stored in a fridge (~6 ℃). Within six hours, the HONO analyses of the dew and blank samples were performed by double-injection in the MARGA in the manual measurement mode as HONO may volatilize between sampling and analysis. For the other

ions (Cl^-, NO_3^-, SO_4^{2-}, Oxalate, Br^- ,F^-, Formate, MSA , PO_4^{3-}, Na^+, NH_4^+, K^+ and Mg^{2+}, Ca^{2+}), the samples were analyzed with laboratory ion chromatogram systems (mod. ICS-3000, Dionex, USA). Blanks from water, the filter, the syringes and bottles were subtracted.

2.5 Aerosol measurements

The particle size distributions were measured in the size range from 5 nm to 10 µm employing by a Dual Mobility Particle Size Spectrometer (TROPOS-type D-MPSS) (Birmili et al., 1999) and an Aerodynamic Particle Size Spectrometer (APSS model 3321, TSI Inc., Shoreview, MN, USA). For the particle number size distribution measurements, the aerosol is sampled through a low flow PM10 inlet and dried in an automatic diffusion dryer (Tuch et al., 2009). The measurements and quality assurance are done following the recommendations given in Wiedensohler et al. (2012) and Wiedensohler et al. (2018). The MPSS derived particle number size distribution was inverted by the algorithm described in Pfeifer et al. (2014), following the bipolar charge distribution of Wiedensohler (1988).

2.6 Other measurements

Trace gases of NO-NO_2-NO_x, SO_2 and O_3 were measured by NO_x analyzer (Thermo Model 42i-TL, Waltham, Massachusetts, USA), SO_2 analyzer APSA-360A and O_3 analyzer APOA 350 E (both Horiba, Kyoto, Japan) with a time resolution of 1 min. It should be noted that NO_2 was converted to NO within the NO_x analyzer by a blue light converter BLC2 (Meteorologie Consult GmbH, Königstein, Germany). The provider for replacement of the Mo-Converter in the 42i-TL analyzer is MLU Messtechnik GmbH, Essen Germany. Meteorological parameters like temperature (T), precipitation, relative humidity (RH) as well as wind velocity and direction were measured by PT1000, a rain gauge (R.M. Young Company, U.S.A.), the CS215 sensor (SensirionAG, Switzerland) and a WindSonic by Gill Instruments (UK), respectively. Global radiation and barometric pressure were recorded by a net radiometer CNR1 (Kipp&Zonen, The Netherlands) and a digital barometer (Vaisala, Germany), respectively.

2.7 Calculation of photolysis rate

Off-line NCAR Tropospheric Ultraviolet and Visible (TUV) transfer model (https://www2.acom.ucar.edu/modeling/tropospheric-ultraviolet-and-visible-tuv-radiation-model) was used to estimate the photolysis rate of HONO (J_{HONO}), NO_2 (J_{NO2}) and production rate of O^1D (J_{O1D}) at the Melpitz station scaled by the measured global radiation. Aerosol optical depth (AOD), total vertical ozone column, total NO_2 column, total cloud optical depth and surface reflectivity (Albedo) were taken from the NASA webpage for the period of measurement (https://neo.sci.gsfc.nasa.gov/blog/).

3 Results

3.1 Inter-comparison of LOPAP and MARGA

The hourly HONO mixing ratio obtained from MARGA with the 30 seconds and hourly averaged HONO mixing ratios from LOPAP are shown in Figure 1a and 1b, respectively. It indicates that the MARGA values were higher than the values of LOPAP but not during the peak events. In addition, the comparison between both instruments in Figure 1a shows a delay of the MARGA concentrations after reaching the maximum concentrations in the morning. This pattern was also observed in previous studies of Volten et al. (2012) and Dammers et al. (2017), who compared miniDOAS instruments with wet denuder systems. Compared to fast responses of the miniDOAS, the denuder-based instruments showed offsets and delays because of inlet memory artefacts by particles or water. Both groups also suggested transport effects of the liquid samples from the sampling to the analysis unit resulting in delays and slow responses.

The comparisons of the MARGA and LOPAP HONO measurements for period M1 and period M2 in Figure 1c result in slopes of 1.57 and 1.66 using error weighted Deming regression, respectively. This result is consistent with the former intercomparison of both instrument types in the Chinese field campaign (Lu et al., 2010;Xu et al., 2019) where the HONO mixing ratio measured with the wet-denuder-ion-chromatography (WD/IC) instrument was affected by a factor of three on average. Within the present work, we evaluated the relative importance of denuder artefact with the inlet artefact. The heterogeneous reactions of NO_2 with H_2O as well as NO_2 with SO_2 in water described by Spindler et al. (2003) or VOCs with NO_2 could explain the artefacts in the denuder solution (Kleffmann and Wiesen, 2008), which could account for ca. 57% (M1, where both LOPAP and MARGA used the common MARGA inlet) of these ca. 66% of overestimated HONO measurement from MARGA. Additional artefacts such as heterogeneous formation of HONO due to the long MARGA inlet system should be responsible for another ca. 9% (the difference between slopes M2 and M1). Hence, the results show that the use of massive sampling inlets, even if they are coated by Teflon, should be avoided for any in-situ HONO instrument. As a result, we chose the LOPAP-measured HONO in the following sections because of its high accuracy.

3.2 General results

Figure 2 and Figure 3 show an overview of the measured HONO, NO, NO_2, O_3, meteorological parameters, water-soluble ions in PM_{10} (NO_3^-, SO_4^{2-}, NH_4^+, Na^+, K^+, Mg^{2+}, Ca^{2+}) and their corresponding trace gases (HONO, HNO_3, SO_2, NH_3) in the present study. The daytime (D, 04:00-18:00, UTC) and nighttime (N, 18:00-04:00) averages are also provided in Table 1. During the two weeks measurement, the prevailing winds were from the southwest

and northwest sectors, indicating a possible influence of city emission from Leipzig, Germany, on the site. The strong wind (maximum 13 m s^{-1}) led to low concentration of water-soluble ions in PM_{10} (NO_3^-, SO_4^{2-}, NH_4^+) and their corresponding trace gases (HNO_3, SO_2, NH_3) during the period April 24th to 29th, 2018. The air temperature ranged from 5 ℃ to 27 ℃ and the RH showed a clear variation pattern with higher levels during the night and lower levels during daytime. In addition, low mixing ratio of NO and NO_2 with a diurnal average of 0.9±1.2 ppbv and 3.7±2.2 ppbv, respectively, were recorded. These observations highlight the nature of our measurement site as a typical background environment. The HONO concentration from the LOPAP measurements varied from 30 pptv to 1582 pptv and showed diurnal variations (with median values of 370±300 pptv and 280±210 pptv during daytime and nighttime, respectively).

Größ et al. (2018) reported the linear function of the global radiation flux vs. OH radical concentration for the campaign EUCAARI 2008 at Melpitz.

$$[OH]=A*Rad \quad \text{(Eq. 1)}$$

with Rad being global solar irradiance in W m^{-2} and [OH] is the hydroxyl radical concentration. The proportionality parameter A is 6110 m^2 W^{-1} cm^{-3}. On the basis of such a correlation, we derived the OH concentration during the period of this field measurement, with an average of $(2.8\pm0.7)\times10^6$ during daytime.

3.3 Diurnal variation of HONO, particles and trace gas species

The diurnal profiles of HONO and related supporting parameters are shown in Figure 4 for the whole period except for two sets of observations: (1) no HONO peak in the morning of April 23rd and (2) HONO peak observed at 0:00-2:00 (UTC) of April 25th (Figure 5). Overall, the HONO increased fast after the sunrise and peaked at 7:00 (UTC), which then dropped rapidly and reached a minimum at around 10:00 (UTC) and kept until 17:00 (UTC). As shown in Figure 4a, 4e and 4f, the early morning variation trend of HONO during daytime was similar to the one of NH_3 in the gas phase as well as NO_3^- and NH_4^+ in PM_{10}. This induced the hypothesis (a) of HONO morning peak might possibly be caused by the photolysis of particle-phase HNO_3/NO_3^- (Ye et al., 2016;Zhou et al., 2003;Zhou et al., 2011). This morning peak of HONO has been reported for Melpitz (April 4th-14th, 2008) by Acker et al. (2004), who expected that the storage of HONO on wet surfaces can be a source for observed daytime HONO. Such daytime pattern was also found in Spain, for a site surround by forests and sandy soils (Sörgel et al., 2011). Sörgel et al. (2011) explained this by local emissions, which are trapped in the stable boundary layer before its breakup of the inversion in the morning based on a similar diurnal cycle for NO and NO_2, which is different with this work. In this work, the NO_2 mixing ratio decreased from the midnight until noon and NO peaked at 5:00 (UTC) then kept low concentration (<1 ppbv) for 18 hours of one day. As reported by

Stemmler et al. (2006), the photosensitized NO_2 on humic acid could act as a source of HONO during the daytime. It was expected that the photosensitized NO_2 on humic acid might lead to a HONO morning peak within hypothesis (b). For hypothesis (c), it was observed that dew was formed overnight during our campaign in Melpitz. Gaseous HONO could be deposited in these droplets. Due to evaporation after sunrise, HONO would be reemitted in the atmosphere and lead to a HONO morning peak. These hypotheses will be further discussed in Section 4.

As shown in Figure 4a and 4b, the HONO and NO_2 concentrations started to increase coincidentally at 16:00 (UTC) when the sunshine was weak. This could be explained by the variation of the vertical mixing increasing the level of all near ground emitted of formed species or the heterogeneous conversion of NO_2 to HONO during nighttime and will be discussed in Section 4. The HONO mixing ratio then decreased from 21:00 (UTC) to around 100 pptv even though the NO_2 concentration kept constant around 5-6 ppbv. This decrease during nighttime indicates the HONO loss process (dry and wet deposition, trapped in the boundary layer or dew etc.) surpassing the HONO formation from the NO_2-to-HONO conversion. The diurnal cycle of O_3 reflects the balance between the photochemical formation of O_3 (e.g. NO_2 + hv) and O_3 consumption (e.g. ozonolysis of terpenes).

3.4 HONO in the dew water

Dew water formation on canopy surfaces could be an efficient removal pathway of water soluble pollutants. High solubility of HONO makes dew water an efficient sink and a stable reservoir for atmospheric HONO. Actually, a lot of dew water has been observed on the grass around the Melpitz station during the sampling period of April 19th to 29th 2018. Hence, to investigate the dissolved HONO in the dew water of Melpitz station, the dew water was collected and analyzed from May 8th to 14th 2019 at the same season like the HONO measurements. Many ions e.g. NO_2^-, Cl^-, NO_3^-, SO_4^{2-}, Oxalate, Br^-, F^-, Formate, MSA, PO_4^{3-}, Na^+, NH_4^+, K^+ and Mg^{2+}, Ca^{2+} were analyzed using MARGA and laboratory IC, but our discussion only focuses on NO_2^-. The sample parameters (time, pH etc.) and NO_2^- concentration in the sample (µg L^{-1}) are shown in Table 2 from two glass plates (plate 1 and plate 2). The final dew water NO_2^- was calculated by subtracting the blank NO_2^- from the raw data of dew water analysis in MARGA. The pH of dew water in Melpitz ranged from 6.30 to 7.00. It should be noted that the dew water was frozen until 1 hour after sunrise on May 8th, 13th and 14th 2019 but not on May 11th 2019. At this day, a third sample was collected sampled from 3:30 to 5:20 (UTC) after collecting the first sample (18:00-3:20 UTC). The NO_2^- concentration per m^2 of the sampler surface (F_{NO2-}) was calculated from the following equation:

$$F_{NO2-} = \frac{[NO_2^-] \times V_{dew}}{S \times 1000} \quad \text{(Eq. 2)}$$

Where $[NO_2^-]$ is the sample concentration in μg L^{-1}, V_{dew} is the sample volume in ml, S is the surface area of the glass sampler as 1.5 m^2. As shown in Table 2, higher F_{NO2-} was obtained on May 11th where dew water was not frozen. On other days (May 8th, May 13th and May 14th) frozen dew water was observed, which likely inhibited HONO to dissolve. Hence, these frozen samples were not considered in this paper. On May 11th, the final F_{NO2^-} could be obtained by averaging F_{NO2^-} of the sum (9.43 μg m^{-2}) of the first and third sample with the second sample (6.40 μg m^{-2}) on 11th May resulting in mean 7.91±2.14 μg m^{-2}. This value will be used for the following calculation and discussion.

4 Discussion

4.1 Contribution of vehicle emissions

Because Melpitz site is close to a main national road from Leipzig to Torgau (Germany) that is within the main southwest wind direction, the contribution of vehicle emissions to the measured HONO mixing ratio should be evaluated. Generally, the HONO/NO_x ratio is usually chosen to derive the emission factor of HONO in the freshly emitted plumes (Kurtenbach et al., 2001). As illustrated in Figure S3, NO_x concentrations were normally lower than 15 ppbv and NO/NO_x ratios were ~0.4 in this campaign, suggesting the detected air is a mixture of fresh and aged air during the measurement period. Therefore, a substantial part of HONO is secondary. Additionally, following the criteria of Li et al. (2018), the bad correlation between HONO and NO_x ($R^2 \approx 0.35$) suggests that the direct HONO emission from the vehicle emitted plumes were less important in this work.

4.2 Nighttime HONO

The nighttime HONO is different to some reported literatures (Huang et al., 2017;Li et al., 2012;Wang et al., 2017;Zhou et al., 2007). HONO increased after sunset to a maximum at 21:00 (UTC) and decreased until sunrise.

4.2.1 Formation through heterogeneous conversion of NO_2

The ratio of HONO/NO_2 is generally used as an index to estimate the efficiency of heterogeneous NO_2-HONO conversion because it is less influenced by transport processes than individual concentrations. However, the ratio might be influenced when a large fraction of HONO is emitted from the traffic but this is expected to be less important as shown in section 4.1. Then in this work, a low emission factor of 0.3% was used to correct the directly HONO emission from vehicles ($HONO_{corr}$) (Kurtenbach et al., 2001) . Six conditions as listed in Table 3 are selected to calculate the NO_2-HONO frequency following the criteria of Li et al. (2018):

(a) only the nighttime data in the absence of sunlight (i.e., 17:30-06:00 UTC) are used;
(b) both $HONO_{corr}$ and $HONO_{corr}$ / NO_2 ratios increased steadily during the target case;
(c) the meteorological conditions, especially surface winds, should be stable.

Figure S4 presents an example of the heterogeneous HONO formation occurring on April 28th, 2018. In this case, the HONO mixing ratios increased rapidly after sunset from 100 pptv to 600 pptv. Together with the HONO mixing ratio, the $HONO_{corr}/NO_2$ ratio increased almost linearly between 18:00 to 19:50 UTC. The slope fitted by the least squares regression for $HONO_{corr}/NO_2$ ratios against time can be taken as the conversion frequency of NO_2-to-HONO (k_{het}).

The ratio of $HONO_{corr}$ / NO_2 ranged from 0.055 to 0.161 with mean value of 0.110±0.041 (Table 3) using the data during early nighttime (17:30-00:00 UTC) in the Melpitz campaign. This mean values are within the wide range of reported values of 0.008-0.13 in the fresh air masses from the most sampling sites (Alicke et al., 2002;Alicke et al., 2003;Sörgel et al., 2011;Su et al., 2008;VandenBoer et al., 2013;Wang et al., 2017;Zhou et al., 2007) except for the study of Yu et al. (2009), who got a high value of 0.3. To our best knowledge, the present work presents also a high NO_2-to-HONO conversion frequency k_{het} of 0.027±0.017 h^{-1} compared with most of the previous studies at urban sites, such as, Alicke et al. (2002) in Milan (0.012 h^{-1}), Wang et al. (2017) in Beijing (0.008 h^{-1}) and Acker and Möller (2007) in Rome (0.01 h^{-1}). However, our value is additionally comparable to Li et al. (2012) with 0.024±0.015 h^{-1}, Alicke et al. (2003) with 0.018±0.009 h^{-1} and Acker and Möller (2007) with 0.027±0.012 h^{-1}, who also conducted rural measurements in the Pearl River Delta (PRD) area in Southern China, Pabstthum in Germany, and Melpitz, respectively, surrounded by farmland (grasses, trees, small forests). The higher value may suggest that a more efficient heterogeneous conversion from NO_2 to HONO is present in rural sites than in urban sites.

4.2.2 Relative importance of particle and ground surface in nocturnal HONO production

The particle surface density S_a was calculated as (5.1-9.9) $\times 10^{-4}$ m^2 m^{-3} from the particle size distribution (Figure S5) ranged from 5 nm to 10 μm of APSS and D-MPSS data by assuming the particle are in spherical shape. The particle surface density S_a was further corrected to be (0.6-1.9) $\times 10^{-3}$ m^2 m^{-3} with a hygroscopic factor $f(RH)$ following the method of Li et al. (2012) and Liu et al. (2008):

$$f(RH)=1+a\times(RH/100)^b \quad \text{(Eq. 3)}$$

where the empirical factors a and b were set to 2.06 and 3.6, respectively.

The formation of HONO through heterogeneous NO_2 conversion on particle surfaces (S_a) can be approximated following the recommendations in Li et al. (2010) by considering 100% HONO yield on the particle surface (NO_2+Org/soot/etc):

$$k_{het} = \frac{1}{4}\gamma_{NO2\rightarrow HONO\_a} \times \upsilon_{NO2} \times \frac{S_a}{V} \quad \text{(Eq. 4)}$$

where υ_{NO2} is the mean molecular velocity of NO_2 (370 m s^{-1}) (Ammann et al., 1998); S_a/V is the particle surface to volume ratio (m^{-1}) representing the surfaces available for heterogeneous reaction, and $\gamma_{NO2\rightarrow HONO\_a}$ is the uptake coefficient of NO_2 at the particle surface. Assuming the entire HONO formation was taking place on the particle surface, the calculated $\gamma_{NO2\rightarrow HONO\_a}$ from the Eq. 4 varied from 2.8×10^{-5} to 3.8×10^{-4} with a mean value of $(1.7\pm1.0)\times10^{-4}$. This theoretical uptake coefficient falls into a reasonable range of 10^{-6} - 10^{-4} similar to former studies (Kleffmann et al., 1998;Kurtenbach et al., 2001;VandenBoer et al., 2013;Wong et al., 2011). However, considering the weak correlations between $HONO_{corr}$ (R^2=0.566), $HONO_{corr}$/ NO_2 (R^2=0.208) and S_a (Figure S6), the relative amount of HONO formed on particle surfaces might be small as previously reported (Kalberer et al., 1999;Sörgel et al., 2011;Wong et al., 2011).

As illustrated above, the heterogeneous NO_2 conversion on ground surfaces (including surfaces such as plants, building, soils etc.) contributes mainly to nighttime formation of HONO, which can be approximated by Eq. 5 following the method in literatures (Kurtenbach et al., 2001;Li et al., 2010;VandenBoer et al., 2013;VandenBoer et al., 2014) and also been applied by Zhang et al. (2016) by considering a 50% HONO yield from R2:

$$k_{het} = \frac{1}{8}\gamma_{NO2\rightarrow HONO\_g} \times \upsilon_{NO2} \times \frac{S_g}{V} \quad \text{(Eq. 5)}$$

where $\gamma_{NO2\rightarrow HONO\_g}$ is the uptake coefficient of NO_2 at the ground surface, S_g/V represents the ground surface to volume ratio. As described by Zhang et al. (2016), the LAI (m^2/m^2) was used to estimate the surface to volume ratio for the vegetation-covered areas, following the method in Sarwar et al. (2008):

$$\frac{S_g}{V} = \frac{2\times LAI}{H} \quad \text{(Eq. 6)}$$

Where H is the mixing layer height, which was calculated from the backward trajectory analysis based on GDAS data under dynamic conditions (Figure S7). The mixing layer height ranged between 20 m and 300 m from 17:00 until around 00:00 UTC in April 2018 (Figure S7). The LAI value is multiplied by a factor of 2 to take the areas on both sides of the leaves into account and is around 4 to 10 for grassland values. In Wohlfahrt et al. (2001), the LAI for meadows with different grass heights are given. Regarding the grass height of ~30 cm in April 2018, we used a factor of 6 in present study. If the entire HONO formation was taking place on the ground surface, the calculated $\gamma_{NO2\rightarrow HONO\_g}$ varied from 2.4×10^{-7} to 3.5×10^{-6} with a mean value of $2.3\pm1.9\times10^{-6}$. This value agrees well with the reported range of $\gamma_{NO2\rightarrow HONO}$ from 10^{-6} to 10^{-5} on the ground surface based on the laboratory studies (Donaldson et al., 2014;VandenBoer et al., 2015) and field campaign in Colorado, USA (VandenBoer et al., 2013) during the night time. It should be noted here that the obtained NO_2 uptake coefficient

on the ground surface is lower than the reactive surface provided by aerosols. As the S/V ratio of particles is typically orders of magnitude lower than for ground surfaces, it is suggested that the heterogeneous reactions of NO_2 on the ground surface may play a dominant role for the nighttime HONO formation.

In addition, the relationship of NO_2-HONO conversion frequency (k_{het} presented in Table 3) with the inverse of wind speed is illustrated in Figure S8a. As indicated in Figure S8a, wind speed was predominantly less than 3 m s^{-1} during the field campaign period in Melpitz. High conversion frequency of NO_2-to-HONO mostly happened when wind speed was less than 1 m s^{-1}, which confirms that HONO formation mainly takes place on the ground. However, one point (in blue in Figure S8a) showed highest NO_2-HONO conversion frequency (k_{het}) when wind speed was ca. 4 m s^{-1} according to the second set of observation mentioned in section 3.3 and Figure 5. The likely reason for the temporary HONO peak is the dew droplet evaporation after increasing wind speed.

4.2.3 HONO deposition on the ground surface

As illustrated in Figure 4a and S4, between midnight and sunrise (22:00-4:00 UTC), the deposition of HONO becomes increasingly important as the absolute amount of HONO decreased. Assuming a constant conversion frequency of NO_2-to-HONO, k_{het}, the HONO deposition rate (L_{HONO}) can be roughly estimated by:

$$L_{HONO}=\frac{d[HONO]}{dt} - k_{het} \times [NO_2] \quad \text{(Eq. 7)}$$

The strength of the HONO sink during night is in average 0.16±0.12 ppbv h^{-1} and ranged from 0.04 to 0.45 ppbv h^{-1}. This value is similar with reported ones in the literature (He et al., 2006).

The relationship of [HONO]/[NO_2] with RH during nighttime (18:00-04:00) is illustrated in Figure S8a. A positive trend of [HONO]/[NO_2] ratio along the RH was found when RH was less than 70%. However, [HONO]/[NO_2] performs a negative trend with RH for values over 70%. The same phenomenon was also observed by Yu et al. (2009) in Kathmandu and Li et al. (2012) in PRD region, China. This finding can be associated with larger amounts of water on various ground surfaces (plants and grasses) when ambient humidity approached saturation, leading to an efficient uptake of HONO.

Assuming all the extra HONO were removed through deposition on the ground surface, the change of HONO in the time interval of 22:00-04:00 (UTC) is parameterized using a combination of Eq. 7 and the following equation:

$$L_{HONO} = \frac{1}{4}\gamma_{HONO,ground} \times [HONO] \times \frac{\upsilon_{HONO,ground}}{H} \quad \text{(Eq. 8)}$$

Where $\gamma_{HONO,ground}$ is the HONO uptake coefficient on the ground surface, $\upsilon_{HONO,ground}$ is the mean molecular velocity of HONO with 3.67×10^4 cm s^{-1}, H is the mixing layer height

calculated from the backward trajectory analysis ranging between 20 m and 150 m with an average of ca. 55 m from 22:00 until 04:00 UTC in April 2018. This approach yielded to a $\gamma_{HONO,ground}$ uptake coefficient in the range of 1.7×10^{-5} to 2.8×10^{-4} with an average of $(1.0\pm0.4)\times10^{-4}$, which is similar to data found in Boulder, Colorado, ranging from 2×10^{-5} to 2×10^{-4} (VandenBoer et al., 2013).

As observed by several studies (He et al., 2006;Rubio et al., 2009;Wentworth et al., 2016), the effective Henry's law solubility of HONO is highly pH-dependent (from borderline soluble at pH = 3 to highly soluble at pH ≥ 6), as would be expected for a weak acid. The pH of collected dew water during nighttime in May 2019 was 6.3-7.0 (Table 2), where the effective Henry's law solubility of HONO would be high. The amount of HONO in this dew water was quantified using MARGA and ranged between 42 and 165 mg L^{-1}, which is higher than NO_2^- in Santiago's dew waters (Rubio et al., 2009). This could strongly support the obtained HONO uptake coefficient on the ground surface. These field-derived surface parameters of nighttime HONO production from NO_2 and surface deposition of HONO are valuable to the model evaluation. However, it should be noted that the measured pH of collected dew from the glass plate might differ compared to the pH of dew found on soil or vegetated surfaces. The chemical nature of the material, with which the water is in contact, can influence the effective pH.

A simple resistance model based on the concept of aerodynamic transport, molecular diffusion and uptake at the surface (presented in SI) as proposed by Huff and Abbatt (2002) was used to evaluate the factor(s) controlling the potential applicability of the γ-coefficients calculated here for the uptake of NO_2 and deposition of HONO. As shown in Figure S9, the deposition loss of HONO is potentially limited by a combination of aerodynamic transport, molecular diffusion and reaction processes. However, the HONO uptake will be transport-limited if the real uptake coefficients are ≥ 2.8×10^{-4} and wind speed was less than 0.5 m s^{-1}. In addition, molecular diffusion could play an important role for HONO uptake on the surface, especially when the winds speed is smaller than ~1 m s^{-1}. Regarding the uptake of NO_2 on the ground surface, the range of NO_2 uptake coefficients as 2.4×10^{-7} to 3.5×10^{-6} obtained in the present work indicates limitation only by the reactive uptake process. The consistency between our findings and the values of these parameters in models (Wong et al., 2011;Zhang et al., 2016) suggests that the broad scale applicability of these field-derived terms for surface conversion of NO_2 should therefore be possible. However, those value of γ found for HONO ($\gamma_{HONO,ground}$=1.7×10^{-5} to 2.8×10^{-4}) require further exploration from various field environments and controlled lab studies.

4.3 Daytime HONO

HONO concentrations started to increase after sunrise and peaked at 7:00 (UTC) (Figure 4),

during that time it also underwent photolysis, eventually reaching a steady state between 10:30–16:30 (UTC). Throughout the day, HONO was observed to reach an averaged minimum mixing ratio of 98±15 pptv. Since NO and NO_2 have not the same diurnal cycle as HONO (Figure 4), the R2 and R7 are not expected to be responsible for this HONO morning peak, but could be the main HONO source for the period of 10:30-16:30 (UTC).

4.3.1 Photostationary state in the gas phase

The measured diurnal daytime HONO could be compared to model results by assuming an instantaneous photo-equilibrium between the gas-phase formation (R7) and gas-phase loss processes (R1 and R11), which is described by the following expression (Kleffmann et al., 2005):

$$[\mathrm{HONO}]_{pss} = \frac{k_7[OH][NO]}{J_{HONO}+k_{11}[OH]} \quad \text{(Eq. 9)}$$

OH concentration was estimated from linear function of the global radiation flux vs. OH radical concentration as described in the previous section and shown in Figure 6, J_{HONO} was calculated using TUV model as described in section 2.6. The rate constants of NO+OH (k_7) and HONO+OH (k_{11}) used are 7.4×10^{-12} cm^3 $molecule^{-1}$ s^{-1} (Burkholder et al., 2015) and 6.0×10^{-12} cm^3 $molecule^{-1}$ s^{-1} (Atkinson et al., 2004), respectively. As a result, shown in Figure 6, the $[HONO]_{pss}$ (Pss, violet curve) could not explain the sudden HONO increase after sunrise but indicates a HONO peak around 4:40 (UTC) according to the relatively high NO concentration. However, some studies (Michoud et al., 2012;Sörgel et al., 2011) already discussed that the stationary state of HONO can be only reached during noontime. Hence, a model calculation (named Model 1) was also used to discuss the HONO contribution from the gas-phase reaction of NO with OH radical.

$$\frac{d[HONO]}{dt} = k_7[OH][NO] + k_{het}[NO_2] - J_{HONO}[HONO] - k_{11}[HONO][OH] \quad \text{(Eq. 10)}$$

k_{het} derived from this work is 0.027 h^{-1}, [NO] and $[NO_2]$ are averaged concentrations from field measurement. The results are shown in Figure 6 (orange line). It is reasonable to indicate that the reaction of R7 only contribute 30-55% to the HONO increase in the early morning (4:30-7:30 UTC). R7 can continually contribute 50% of the measured HONO from 10:30 to 16:30 (UTC). However, regarding on the large uncertainty of [OH] (a factor of 2), the "unknown HONO sources" exist but could be not crucial. Basically, the additional HONO contribution rate could be estimated from the following equation:

$$P_{unknown} = \frac{d[HONO]}{dt} + J_{HONO}[HONO] + k_{11}[OH][HONO] - k_7[OH][NO] \quad \text{(Eq. 11)}$$

An additional source of 91±41 pptv h^{-1} was derived beside OH reaction with NO according to a HONO mixing ratio 98±15 pptv for the time period of 10:30 to 16:30 (UTC). This could be well explained by the photochemical processes such as R5 and R9 and would be discussed

deeply in the next section.

4.3.2 Evidence for nighttime deposited HONO as a morning source

As observed in our field measurement and shown in Figure 2, the HONO concentrations always presented a strong increase from 4:00 – 7:00 (UTC), which induces three hypotheses as also mentioned in section 3.3: (a) photolysis of gas-phase and particulate nitrate, (b) photosensitized conversion of NO_2, (c) dew on ground surfaces served as HONO sink during the night and become a morning source by releasing the trapped nitrite back into ambient air. To identify this HONO source, the chemical box model as expressed in Eq. 12 was extended with additional processes. Heterogeneous reaction of NO_2 on the wet surface (R2) and HONO deposition on the ground surface were firstly used to quantify the contributions of the well-known HONO production and loss processes. In addition, the HONO deposition on the ground surface independent on RH (24 hours, named Model 2) and with RH dependence (nighttime 17:00-8:00 UTC, named Model 3) are also discussed.

$$\frac{d[HONO]}{dt} = k_7[OH][NO] + k_{het}[NO_2] - J_{HONO}[HONO] - k_{11}[HONO][OH] - \frac{1}{4}\gamma_{HONO,ground}[HONO]\frac{\upsilon_{HONO,ground}}{H} \quad \text{(Eq. 12)}$$

Both the surface production of HONO through NO_2 heterogeneous reaction and subsequent loss by ground surface deposition are already termed in Eq. 5 and Eq. 8, respectively. Here, k_{het} is 0.027 h^{-1} and $\gamma_{HONO,ground}$ is $(1.0 \pm 0.4) \times 10^{-4}$ calculated from the present observations. These values are applied to the model calculation to simulate the diurnal cycle of HONO. As shown in Figure 6, both Model 2 (blue line) and Model 3 (green square) cannot explain the HONO morning peak but Model 3 can well reproduce the nighttime HONO indicating that surface loss of HONO is an important sink to consider when the RH was saturated. Hence, Model 3 was used as basic run for the following model calculation.

To investigate the contribution of photolysis of nitric acid and nitrate (HNO_3/NO_3^-) (R9) on the diurnal HONO based on the hypothesis (a), the following model calculation (Model 4, pink line) was made:

$$\frac{d[HONO]}{dt} = k_7[OH][NO] + k_{het}[NO_2] + J_{HNO3}[HNO_3/NO_3^-] - J_{HONO}[HONO] - k_{11}[HONO][OH] - \frac{1}{4}\gamma_{HONO,ground}[HONO]\frac{\upsilon_{HONO,ground}}{H} \quad \text{(Eq. 13)}$$

Here gas-phase HNO_3 and particle NO_3^- are summed up and the photolysis frequency J_{HNO3} was derived from the TUV model by multiplying an enhanced factor of 30 due to a faster photolysis of particle-phase HNO_3 (Romer et al., 2018). As a result, the photolysis of HNO_3/NO_3^- (Model 4, pink line) could not reproduce the HONO morning peak shown in Figure 6. However, it could well reproduce the HONO for the time period of 10:30 to 16:30

(UTC).

To investigate the contribution of photosensitized conversion of NO_2 (R5) on the diurnal HONO based on the hypothesis (b), the following model calculation (Model 5) was performed:

$$\frac{d[HONO]}{dt} = k_7[OH][NO] + k_{het}[NO_2] + \frac{1}{4}(\gamma_a\frac{S_a}{V} + \gamma_g\frac{S_g}{V})\upsilon_{NO2}J_{NO2}[NO_2] - J_{HONO}[HONO] - k_{11}[HONO][OH] - \frac{1}{4}\gamma_{HONO,ground}[HONO]\frac{\upsilon_{HONO,ground}}{H} \quad \text{(Eq. 14)}$$

Here the γ_a and γ_g are the light-enhanced NO_2 uptake coefficients both of 2.0×10^{-5} (Zhang et al., 2016) on both the aerosol surface and ground surface, respectively. J_{NO2} was multiplied with $\frac{light\ intensity}{400}$ when the light intensity is ≥ 400 W m^{-2}. As shown in Figure 6 (Model 5, cyan line), the photosensitized NO_2 on the aerosol and ground surface could not reproduce the HONO morning peak. This favors the third hypothesis that dew evaporation processes release HONO resulting in the sudden morning peak.

Indeed, as shown in Figure S10, the HONO morning peak always happens according to a fast decrease of RH between 4:30-9:00 (UTC). However, there is one case happened at 1:00 (UTC) on April 25th, 2018, possibly due to an upcoming strong wind which decreased the RH and evaporated the dew water on the ground surface. It should be noted that this HONO morning peak was never observed during this field measurement period without a fast RH decrease, in case of dry ground surface as it was observed during the morning of April 23rd, 2018. To figure out the relationship between temporary HONO emission from dew water and decreasing RH, the following equation was defined:

$$k_{emission} = \frac{d(\frac{HONO_{unknown}}{99.5-RH})}{dt} = \frac{\frac{HONO_{unknown}}{99.5-RH}(t_2) - \frac{HONO_{unknown}}{99.5-RH}(t_1)}{(t_2 - t_1)} \quad \text{(Eq. 15)}$$

where $HONO_{unknown} = HONO_{measure} - HONO_{Model4}$ was calculated for each day in the whole campaign period. $k_{emission}$ could be obtained from the linear least square analysis of $\frac{HONO_{unknown}}{99.5-RH}$ vs. the internal time of HONO morning peak (4:30-7:00, UTC) as shown in Figure 7. The maximum and minimum of $k_{emission}$ are obtained as 0.026±0.008 and 0.006±0.001 pptv $\%^{-1}$ s^{-1}, respectively, with an average of 0.016±0.014 pptv $\%^{-1}$ s^{-1} as presented in Table 4. The average value was used in the following model calculation to reproduce the diurnal cycle of HONO.

$$\frac{d[HONO]}{dt} = k_7[OH][NO] + k_{het}[NO_2] + J_{HNO3}[HNO_3/NO_3^-] + \frac{1}{4}(\gamma_a\frac{S_a}{V} + \gamma_g\frac{S_g}{V})\upsilon_{NO2}J_{NO2}[NO_2] + k_{emission}*(99.5\text{-}RH) - J_{HONO}[HONO] - k_{11}[HONO][OH] - \frac{1}{4}\gamma_{HONO,ground}[HONO]\frac{\upsilon_{HONO,groud}}{H} \quad \text{(Eq. 16)}$$

In Figure 6, the Model 6 (red line) shows that the amount of deposited HONO could

represent the amount of HONO during the morning peak. In Figure S11, the measured atmospheric HONO mixing ratio and the calculated HONO mixing ratio using model 6 with a minimum dew HONO emission ($k_{emission}$ = 0.006 pptv $\%^{-1}$ s^{-1}) and a maximum dew HONO emission ($k_{emission}$ = 0.026 pptv $\%^{-1}$ s^{-1}) is shown. HONO emission from the dew water evaporation represented at least 90% and likely in excess of 100% of the calculated unknown HONO morning peak, which may continually serve as HONO source for the whole daytime as long as water evaporates depending on the weather condition.

4.3.3 HONO emission from dew water evaporation in the morning

The hypothetical morning HONO mixing ratio (pptv) due to the complete dew water evaporation could be estimated from the following equation by taking the measured dew nitrite and the mixing layer height:

$$[HONO] = \frac{\alpha \times S_g \times F_{NO2-}}{H \times S_g} = \frac{\alpha \times F_{NO2-}}{H} \quad \text{(Eq. 17)}$$

F_{NO2}^- is the NO_2^- concentration per m^2 of the glass sampler surface. The mean F_{NO2-} from May 11th 2019 was used for the calculation. S_g represents the surface area of the flat ground (analog to the surface area of the glass sampler), α is the enhanced factor for V_{dew} (dew water sample volume of the glass sampler in Eq.2) due to the larger cold surfaces from grass which can get in contact with humid air than the flat glass sampler. α was calculated as 2×LAI to take the areas on both sides of the leaves and the vegetation-covered areas on the ground into account. Regarding the grass height during the dew measurements (~30cm) that is approximately the height in April 2018 and May 2019, we used a factor of 6 for LAI. During the HONO peak at 6 or 7 UTC, the mixing height ranged between 175 m and 600 m, while the value ranged from 20 m to 200 m at 0:00 – 5:00 UTC. Hence, the overall concentration increase from this source would be 2264±612, 1132±306, 453±122, 226±61 and 76±20 pptv, if all of the deposited HONO is released into the overlying air column for a mixing height of 20, 40, 100, 200 and 600 m, respectively. Since the released HONO was subjected to photolysis, using a J_{HONO} from TUV model scaled by global radiation (section 2.7), a maximum [HONO] of 1053±45, 527±22, 211±9, 105±4 and 35±1 pptv for the mixing height 20, 40, 100, 200 and 600 m, respectively, would be contributed from the surface nitrite release at 7:00 UTC after the process started from 4:00 UTC. For a reasonable 100 m mixing height, this would account for ~30% of the observed HONO morning peak in Figure 6. This low percentage might be a result of the different sampling time of dew measurement compared with HONO measurement. Although the above calculations may be well simplified, the results do suggest that the release of the deposited HONO on wet/moist canopy surfaces may contribute to the morning HONO concentrations in the overlying atmosphere right after dew evaporation.

Indeed, few field studies (He et al., 2006;Rubio et al., 2009) have reported that dew water can serve as a sink and a temporary reservoir of atmospheric HONO. Previously, the role of dew as a nighttime reservoir and morning source for atmospheric NH_3 has been reported by Wentworth et al. (2016). Our results suggest that nocturnally deposited HONO forms a ground surface reservoir, which can be released in the following morning by dew evaporation. Therefore, a significant fraction of the daytime HONO source can be explained for the Melpitz observations.

4.3.4 Impact on the primary OH sources

HONO serves as an important primary source of OH during daytime in the troposphere (Kanaya et al., 2007;Kleffmann et al., 2005;Villena et al., 2011). Seiler et al. (2012) reported that the HONO is almost the only source of OH radicals in the early morning. The morning peak of HONO is mainly released from the dew evaporation and could imply a strong supply of OH radicals and, hence, enhances atmospheric oxidizing capacity in the atmosphere around Melpitz. Here, the net rate of OH radical from the HONO photolysis was calculated and compared with that from ozone photolysis, which is typically proposed as the major OH radical source in the atmosphere where water vapor is not limited.

$O_3 + h\nu \rightarrow O(^1D) + O_2$ (λ <320 nm) (R12)

$O(^1D) + H_2O \rightarrow 2OH$ (R13)

$O(^1D) + M \rightarrow O(^3P) + M$ (M =N_2) (R14)

Other OH sources, such as photolysis of oxidized VOCs, peroxides and ozonolysis of unsaturated VOCs are not considered due to the lack of measurement data for these radical precursors. The net rate of OH production from HONO photolysis ($P_{HONO->OH}$) was calculated by the source strength subtracting the sink terms due to reactions of R7 and R11. The OH production rate ($P_{O3->OH}$) from O_3 photolysis can be calculated by using the method proposed by Su et al. (2008) and Li et al. (2018).

$$P_{HONO->OH} = J_{HONO}[HONO] - k_7[NO][OH] - k_{11}[HONO][OH] \quad \text{(Eq. 18)}$$

$$P_{O3->OH} = 2J(O^1D)[O_3]\left(\frac{k_{13}[H_2O]}{k_{14}[M]+k_{13}[H_2O]}\right) \quad \text{(Eq. 19)}$$

Where $J(O^1D)$ was obtained from the TUV model scaled by the global radiation. The temperature dependence of k_{13} and k_{14} are taken from JPL/NASA Evaluation Number 18 (Burkholder et al., 2015). As shown in Figure 8, the photolysis of HONO produced similar amounts of OH compared with photolysis of ozone at the mean daytime (9:00-14:00, UTC), as $(7.2 \pm 2.0) \times 10^5$ molecule cm^{-3} s^{-1}. $P_{O3->OH}$ was, as expected, highest during the highest J values and negligible at the sunrise and sunset. $P_{HONO->OH}$ had a similar trend after the noontime but presented a strong OH production around 7:00 (UTC) due to the HONO morning peak. These results demonstrate the significant role of HONO in the atmospheric

oxidizing capacity, especially for areas that experience frequent dew formation. In addition, the OH concentration calculated from the global radiation flux measurement was also shown in yellow color in Figure 8. The different trend of calculated OH concentration compared with P_{HONO} indicate that the morning OH concentration could be highly underestimated.

5 Conclusion and Atmospheric Implications

The inter-comparison of MARGA and LOPAP for the HONO measurement was applied from April 19th to 29th, 2018 at the Melpitz site. Higher HONO mixing ratio (ca. 66%) was obtained from MARGA compared with that of LOPAP caused by heterogeneous reactions within the MARGA WRD or potential sampling inlet artefact.

The maximum dew water NO_2^- concentration per m^2 of glass sampler surface was determined to be 7.91 ± 2.14 µg m^{-2}in May 2019. Thus, under consideration of photolytical losses and homogeneous mixing, the maximum contribution to the HONO morning peak from dew water evaporation could be calculated and ranged from 1053 ± 45 to 35 ± 1 pptv for mixing height of 20 to 600 m, respectively.

Well-defined diurnal cycles of HONO with concentration peaks in the early morning and in the evening are found. High time resolution of HONO measurements revealed (i) the vehicle emission is a negligible HONO source at the Melpitz site; (ii) HONO formed from the heterogeneous reaction NO_2 on the ground surface is the dominant nighttime source with a high NO_2-HONO conversion frequency of 0.027 ± 0.017 h^{-1}; (iii) significant amounts of HONO (0.16 ± 0.12 ppbv h^{-1}) deposited to the ground surface at night. The accurate observations of HONO and NO_2 allowed direct evaluation of the ground uptake coefficients for these species at night: $\gamma_{NO2 \rightarrow HONO\_g} = 2.4 \times 10^{-7}$ to 3.5×10^{-6}, $\gamma_{HONO,ground} = 1.7 \times 10^{-5}$ to 2.8×10^{-4}. The ground uptake coefficient of NO_2 and HONO are within the ranges of laboratory and model coefficients. The range of HONO uptake coefficient values calculated in this investigation are potentially limited by a combination of transport and diffusion to the ground surface.

A chemical model utilizing observational constraints on the HONO chemical system and known sources and sinks support the hypothesis that dew water on the ground surface, especially on leaf surfaces, behave as a sink at night and a temporary reservoir for atmospheric HONO in the morning. The dew evaporation had a negative relationship with the RH in the atmosphere and, hence, the HONO emission rate was estimated to be 0.016 ± 0.014 pptv $\%^{-1}$ s^{-1} dependent on the RH after sunrise (start from 4:00, UTC). Furthermore, the formation and evaporation of dew on the ground surface influence significantly the air-surface exchange of HONO and, thus, its temporal distributions in the atmospheric boundary layer in the morning and night. The OH production rate from the photolysis of HONO compared with that from photolysis of O_3 showed that this dew emission

of HONO can strongly enhance the OH reactivity throughout morning time and, hence, plays a vital role in the atmospheric oxidation.

740

Author contributions

RY wrote the paper with input from all authors. BS and GS analyzed the MARGA and dew data and wrote the paper. RY and BG conducted the HONO measurement using LOPAP. TT and AW were responsible for the particle measurement. AM and HH designed the
745 experiments and lead the campaign. All co-authors commented on the manuscript.

Competing interests

The authors declare to have no competing interests.

750 **Acknowledgements**

The authors acknowledge financial support of this study and deployment of the MARGA system by the German Federal Environment Agency (UBA) research foundation under contracts No:351 01 093 and 351 01 070, as well as the European Union (EU) for the Transnational access (TNA) under ACTRIS-2: Comparison of HONO-measurements with
755 MARGA and LOPAP at TROPOS research-site Melpitz (MARLO) is part of the project that has received funding from the European Union's Horizon 2020 research and innovation programme under grant agreement No 654109. For the laboratory analysis and the preparation of solutions, we thank A. Dietze, A. Rödger and S. Fuchs. For the support especially in the field, we thank R. Rabe and A. Grüner. We thank also the TROPOS mechanical workshop for
760 the construction of the dew sampler. The CNRS team (Orléans-France) acknowledges the support from Labex Voltaire (ANR-10-LABX-100-01) and ARD PIVOTS program (supported by the Centre-Val de Loire regional council). Europe invests in Centre-Val de Loire with the European Regional Development Fund.

References

Acker, K., Spindler, G., and Brüggemann, E.: Nitrous and nitric acid measurements during the INTERCOMP2000 campaign in Melpitz, Atmos. Environ., 38, 6497-6505, 10.1016/j.atmosenv.2004.08.030, 2004.

Acker, K., and Möller, D.: Corrigendum to: Atmospheric variation of nitrous acid at different sites in Europe, Environ. Chem., 4, 364-364, https://doi.org/10.1071/EN07023_CO, 2007.

Alicke, B., Platt, U., and Stutz, J.: Impact of nitrous acid photolysis on the total hydroxyl radical budget during the Limitation of Oxidant Production/Pianura Padana Produzione di Ozono study in Milan, J. Geophys. Res. Atmos., 107, 8196, doi:10.1029/2000JD000075, 2002.

Alicke, B., Geyer, A., Hofzumahaus, A., Holland, F., Konrad, S., Pätz, H. W., Schäfer, J., Stutz, J., Volz-Thomas, A., and Platt, U.: OH formation by HONO photolysis during the BERLIOZ experiment, J. Geophys. Res. Atmos., 108, 8247, doi:10.1029/2001JD000579, 2003.

Ammann, M., Kalberer, M., Jost, D. T., Tobler, L., Rössler, E., Piguet, D., Gäggeler, H. W., and Baltensperger, U.: Heterogeneous production of nitrous acid on soot in polluted air masses, Nature, 395, 157, 10.1038/25965, 1998.

Ammann, M., Rössler, E., Strekowski, R., and George, C.: Nitrogen dioxide multiphase chemistry: Uptake kinetics on aqueous solutions containing phenolic compounds, Phys. Chem. Chem. Phys., 7, 2513-2518, 10.1039/B501808K, 2005.

Arens, F., Gutzwiller, L., Baltensperger, U., Gäggeler, H. W., and Ammann, M.: Heterogeneous Reaction of NO2 on Diesel Soot Particles, Environ. Sci. Technol., 35, 2191-2199, 10.1021/es000207s, 2001.

Atkinson, R., Baulch, D. L., Cox, R. A., Crowley, J. N., Hampson, R. F., Hynes, R. G., Jenkin, M. E., Rossi, M. J., and Troe, J.: IUPAC Task Group on Atmospheric Chemical Kinetic Data Evaluation, Atmos. Chem. Phys., 4, 1461-1738, 2004.

Aubin, D. G., and Abbatt, J. P. D.: Interaction of NO_2 with Hydrocarbon Soot: Focus on HONO Yield, Surface Modification, and Mechanism, J. Phys. Chem. A, 111, 6263-6273, 10.1021/jp068884h, 2007.

Bernard, F., Cazaunau, M., Grosselin, B., Zhou, B., Zheng, J., Liang, P., Zhang, Y. J., Ye, X. N., Daële, V., Mu, Y. J., Zhang, R. Y., Chen, J. M., and Mellouki, A.: Measurements of nitrous acid (HONO) in urban area of Shanghai, China, Environmental Science and Pollution Research, 23, 5818-5829, 10.1007/s11356-015-5797-4, 2016.

Birmili, W., Stratmann, F., and Wiedensohler, A.: Design of a DMA-based size spectrometer for a large particle size range and stable operation, J Aerosol Sci, 30, 549-553, 10.1016/S0021-8502(98)00047-0, 1999.

Burkholder, J. B., P. Sander, S., Abbatt, J., Barker, J. R., Huie, R. E., Kolb, C. E., Kurylo, M. J., Orkin, V. L., Wilmouth, D. M., and Wine, P. H.: Chemical Kinetics and Photochemical Data for Use in Atmospheric Studies, Evaluation No. 18, in, edited by: JPL Publication 15-10, J. P. L., Pasadena,, 2015.

Dammers, E., Schaap, M., Haaima, M., Palm, M., Kruit, R. J. W., Volten, H., Hensen, A., Swart, D., and Erisman, J. W.: Measuring atmospheric ammonia with remote sensing

campaign: Part 1-Characterisation of vertical ammonia concentration profile in the centre of The Netherlands, Atmos. Environ., 169, 97-112, 10.1016/j.atmosenv.2017.08.067, 2017.

Donaldson, M. A., Berke, A. E., and Raff, J. D.: Uptake of Gas Phase Nitrous Acid onto Boundary Layer Soil Surfaces, Environ. Sci. Technol., 48, 375-383, 10.1021/es404156a, 2014.

Febo, A., Perrino, C., and Cortiello, M.: A denuder technique for the measurement of nitrous acid in urban atmospheres, Atmos. Environ., 27, 1721-1728, 10.1016/0960-1686(93)90235-q, 1993.

Finlayson-Pitts, B. J., Wingen, L. M., Sumner, A. L., Syomin, D., and Ramazan, K. A.: The heterogeneous hydrolysis of NO_2 in laboratory systems and in outdoor and indoor atmospheres: An integrated mechanism, Phys. Chem. Chem. Phys., 5, 223-242, 10.1039/B208564J, 2003.

Finlayson-Pitts, B. J.: Reactions at surfaces in the atmosphere: integration of experiments and theory as necessary (but not necessarily sufficient) for predicting the physical chemistry of aerosols, Phys. Chem. Chem. Phys., 11, 7760-7779, 10.1039/b906540g, 2009.

Gerecke, A., Thielmann, A., Gutzwiller, L., and Rossi, M. J.: The chemical kinetics of HONO formation resulting from heterogeneous interaction of NO2 with flame soot, Geophysical Research Letters, 25, 2453-2456, 10.1029/98gl01796, 1998.

Größ, J., Hamed, A., Sonntag, A., Spindler, G., Manninen, H. E., Nieminen, T., Kulmala, M., Hõrrak, U., Plass-Dülmer, C., Wiedensohler, A., and Birmili, W.: Atmospheric new particle formation at the research station Melpitz, Germany: connection with gaseous precursors and meteorological parameters, Atmos. Chem. Phys., 18, 1835-1861, 10.5194/acp-18-1835-2018, 2018.

Gustafsson, R. J., Kyriakou, G., and Lambert, R. M.: The molecular mechanism of tropospheric nitrous acid production on mineral dust surfaces, ChemPhysChem, 9, 1390-1393, 10.1002/cphc.200800259, 2008.

Gutzwiller, L., Arens, F., Baltensperger, U., Gäggeler, H. W., and Ammann, M.: Significance of Semivolatile Diesel Exhaust Organics for Secondary HONO Formation, Environ. Sci. Technol., 36, 677-682, 10.1021/es015673b, 2002.

He, Y., Zhou, X., Hou, J., Gao, H., and Bertman, S. B.: Importance of dew in controlling the air-surface exchange of HONO in rural forested environments, Geophys. Res. Lett., 33, doi:10.1029/2005GL024348, 2006.

Heland, J., Kleffmann, J., Kurtenbach, R., and Wiesen, P.: A New Instrument To Measure Gaseous Nitrous Acid (HONO) in the Atmosphere, Environ. Sci. Technol., 35, 3207-3212, 10.1021/es000303t, 2001.

Huang, G., Zhou, X. L., Deng, G. H., Qiao, H. C., and Civerolo, K.: Measurements of atmospheric nitrous acid and nitric acid, Atmos. Environ., 36, 2225-2235, 10.1016/s1352-2310(02)00170-x, 2002.

Huang, R. J., Yang, L., Cao, J. J., Wang, Q. Y., Tie, X. X., Ho, K. F., Shen, Z. X., Zhang, R. J., Li, G. H., Zhu, C. S., Zhang, N. N., Dai, W. T., Zhou, J. M., Liu, S. X., Chen, Y., Chen, J., and O'Dowd, C. D.: Concentration and sources of atmospheric nitrous acid (HONO) at an urban site in Western China, Sci. Total Environ., 593, 165-172, 10.1016/j.scitotenv.2017.02.166, 2017.

Huff, A. K., and Abbatt, J. P. D.: Kinetics and Product Yields in the Heterogeneous Reactions of HOBr with Ice Surfaces Containing NaBr and NaCl, J. Phys. Chem. A, 106, 5279-5287, 10.1021/jp014296m, 2002.

Kalberer, M., Ammann, M., Arens, F., Gäggeler, H. W., and Baltensperger, U.: Heterogeneous formation of nitrous acid (HONO) on soot aerosol particles, J. Geophys. Res. Atmos., 104, 13825-13832, doi:10.1029/1999JD900141, 1999.

Kanaya, Y., Cao, R., Akimoto, H., Fukuda, M., Komazaki, Y., Yokouchi, Y., Koike, M., Tanimoto, H., Takegawa, N., and Kondo, Y.: Urban photochemistry in central Tokyo: 1. Observed and modeled OH and HO2 radical concentrations during the winter and summer of 2004, J. Geophys. Res. Atmos., 112, doi:10.1029/2007JD008670, 2007.

Kanda, Y., and Taira, M.: Chemiluminescent method for continuous monitoring of nitrous acid in ambient air, Anal. Chem., 62, 2084-2087, 10.1021/ac00218a007, 1990.

Kleffmann, J., Becker, K. H., and Wiesen, P.: Heterogeneous NO_2 conversion processes on acid surfaces: Possible atmospheric implications, Atmos. Environ., 32, 2721-2729, 10.1016/s1352-2310(98)00065-x, 1998.

Kleffmann, J., Gavriloaiei, T., Hofzumahaus, A., Holland, F., Koppmann, R., Rupp, L., Schlosser, E., Siese, M., and Wahner, A.: Daytime formation of nitrous acid: A major source of OH radicals in a forest, Geophys. Res. Lett., 32, doi:10.1029/2005GL022524, 2005.

Kleffmann, J., Lörzer, J. C., Wiesen, P., Kern, C., Trick, S., Volkamer, R., Rodenas, M., and Wirtz, K.: Intercomparison of the DOAS and LOPAP techniques for the detection of nitrous acid (HONO), Atmos. Environ., 40, 3640-3652, https://doi.org/10.1016/j.atmosenv.2006.03.027, 2006.

Kleffmann, J., and Wiesen, P.: Technical Note: Quantification of interferences of wet chemical HONO LOPAP measurements under simulated polar conditions, Atmos. Chem. Phys., 8, 6813-6822, 10.5194/acp-8-6813-2008, 2008.

Kurtenbach, R., Becker, K. H., Gomes, J. A. G., Kleffmann, J., Lörzer, J. C., Spittler, M., Wiesen, P., Ackermann, R., Geyer, A., and Platt, U.: Investigations of emissions and heterogeneous formation of HONO in a road traffic tunnel, Atmos. Environ., 35, 3385-3394, 10.1016/s1352-2310(01)00138-8, 2001.

Lahoutifard, N., Ammann, M., Gutzwiller, L., Ervens, B., and George, C.: The impact of multiphase reactions of NO_2 with aromatics: a modelling approach, Atmos. Chem. Phys., 2, 215-226, 10.5194/acp-2-215-2002, 2002.

Lammel, G., and Perner, D.: The atmospheric aerosol as a source of nitrous acid in the polluted atmosphere, J. Aerosol Sci., 19, 1199-1202, https://doi.org/10.1016/0021-8502(88)90135-8, 1988.

Lammel, G., and Cape, J. N.: Nitrous acid and nitrite in the atmosphere, Chem. Soc. Rev., 25, 361-369, 10.1039/CS9962500361, 1996.

Li, D., Xue, L., Wen, L., Wang, X., Chen, T., Mellouki, A., Chen, J., and Wang, W.: Characteristics and sources of nitrous acid in an urban atmosphere of northern China: Results from 1-yr continuous observations, Atmos. Environ., 182, 296-306, https://doi.org/10.1016/j.atmosenv.2018.03.033, 2018.

Li, G., Lei, W., Zavala, M., Volkamer, R., Dusanter, S., Stevens, P., and Molina, L. T.: Impacts of HONO sources on the photochemistry in Mexico City during the

MCMA-2006/MILAGO Campaign, Atmos. Chem. Phys., 10, 6551-6567, 10.5194/acp-10-6551-2010, 2010.

Li, X., Brauers, T., Häseler, R., Bohn, B., Fuchs, H., Hofzumahaus, A., Holland, F., Lou, S., Lu, K. D., Rohrer, F., Hu, M., Zeng, L. M., Zhang, Y. H., Garland, R. M., Su, H., Nowak, A., Wiedensohler, A., Takegawa, N., Shao, M., and Wahner, A.: Exploring the atmospheric chemistry of nitrous acid (HONO) at a rural site in Southern China, Atmos. Chem. Phys., 12, 1497-1513, 10.5194/acp-12-1497-2012, 2012.

Liu, X., Cheng, Y., Zhang, Y., Jung, J., Sugimoto, N., Chang, S.-Y., Kim, Y. J., Fan, S., and Zeng, L.: Influences of relative humidity and particle chemical composition on aerosol scattering properties during the 2006 PRD campaign, Atmos. Environ., 42, 1525-1536, https://doi.org/10.1016/j.atmosenv.2007.10.077, 2008.

Lu, K., Zhang, Y., Su, H., Brauers, T., Chou, C. C., Hofzumahaus, A., Liu, S. C., Kita, K., Kondo, Y., Shao, M., Wahner, A., Wang, J., Wang, X., and Zhu, T.: Oxidant (O_3 + NO_2) production processes and formation regimes in Beijing, Journal of Geophysical Research: Atmospheres, 115, 10.1029/2009jd012714, 2010.

Michoud, V., Kukui, A., Camredon, M., Colomb, A., Borbon, A., Miet, K., Aumont, B., Beekmann, M., Durand-Jolibois, R., Perrier, S., Zapf, P., Siour, G., Ait-Helal, W., Locoge, N., Sauvage, S., Afif, C., Gros, V., Furger, M., Ancellet, G., and Doussin, J. F.: Radical budget analysis in a suburban European site during the MEGAPOLI summer field campaign, Atmos. Chem. Phys., 12, 11951-11974, 10.5194/acp-12-11951-2012, 2012.

Monge, M. E., D'Anna, B., Mazri, L., Giroir-Fendler, A., Ammann, M., Donaldson, D. J., and George, C.: Light changes the atmospheric reactivity of soot, Proceedings of the National Academy of Sciences, 107, 6605-6609, 10.1073/pnas.0908341107, 2010.

Pagsberg, P., Bjergbakke, E., Ratajczak, E., and Sillesen, A.: Kinetics of the gas phase reaction OH + NO(+M)→HONO(+M) and the determination of the UV absorption cross sections of HONO, Chem. Phys. Lett., 272, 383-390, https://doi.org/10.1016/S0009-2614(97)00576-9, 1997.

Pfeifer, S., Birmili, W., Schladitz, A., Müller, T., Nowak, A., and Wiedensohler, A.: A fast and easy-to-implement inversion algorithm for mobility particle size spectrometers considering particle number size distribution information outside of the detection range, Atmos. Meas. Tech., 7, 95-105, 10.5194/amt-7-95-2014, 2014.

Platt, U., Perner, D., Harris, G. W., Winer, A. M., and Pitts, J. N.: Observations of nitrous acid in an urban atmosphere by differential optical absorption, Nature, 285, 312-314, 10.1038/285312a0, 1980.

Romer, P. S., Wooldridge, P. J., Crounse, J. D., Kim, M. J., Wennberg, P. O., Dibb, J. E., Scheuer, E., Blake, D. R., Meinardi, S., Brosius, A. L., Thames, A. B., Miller, D. O., Brune, W. H., Hall, S. R., Ryerson, T. B., and Cohen, R. C.: Constraints on Aerosol Nitrate Photolysis as a Potential Source of HONO and NOx, Environmental Science & Technology, 52, 13738-13746, 10.1021/acs.est.8b03861, 2018.

Rubio, M. A., Lissi, E., Villena, G., Elshorbany, Y. F., Kleffmann, J., Kurtenbach, R., and Wiesen, P.: Simultaneous measurements of formaldehyde and nitrous acid in dews and gas phase in the atmosphere of Santiago, Chile, Atmos. Environ., 43, 6106-6109, 10.1016/j.atmosenv.2009.09.017, 2009.

Sörgel, M., Regelin, E., Bozem, H., Diesch, J.-M., Drewnick, F., Fischer, H., Harder, H., Held,

A., Hosaynali-Beygi, Z., Martinez, M., and Zetzsch, C.: Quantification of the unknown HONO daytime source and its relation to NO_2, Atmos. Chem. Phys., 11, 10433-10447, 10.5194/acp-11-10433-2011, 2011.

Sarwar, G., Roselle, S. J., Mathur, R., Appel, W., Dennis, R. L., and Vogel, B.: A comparison of CMAQ HONO predictions with observations from the Northeast Oxidant and Particle Study, Atmospheric Environment, 42, 5760-5770, https://doi.org/10.1016/j.atmosenv.2007.12.065, 2008.

Schiller, C. L., Locquiao, S., Johnson, T. J., and Harris, G. W.: Atmospheric measurements of HONO by tunable diode laser absorption spectroscopy, J. Atmos. Chem., 40, 275-293, 10.1023/a:1012264601306, 2001.

Seiler, W., Becker, K.-H., and Schaller, E.: Tropospheric Chemistry: Results of the German Tropospheric Chemistry Programme, Springer Netherlands, 2012.

Spindler, G., Hesper, J., Brüggemann, E., Dubois, R., Müller, T., and Herrmann, H.: Wet annular denuder measurements of nitrous acid: laboratory study of the artefact reaction of NO_2 with S(IV) in aqueous solution and comparison with field measurements, Atmos. Environ., 37, 2643-2662, 10.1016/s1352-2310(03)00209-7, 2003.

Spindler, G., Müller, T., Brüggemann, E., Gnauk, T., and Herrmann, H.: Long-term size-segregated characterization of PM_{10}, $PM_{2.5}$, and PM_1 at the IfT research station Melpitz downwind of Leipzig (Germany) using high and low-volume filter samplers, Atmos. Environ., 38, 5333-5347, 10.1016/j.atmosenv.2003.12.047, 2004.

Stemmler, K., Ammann, M., Donders, C., Kleffmann, J., and George, C.: Photosensitized reduction of nitrogen dioxide on humic acid as a source of nitrous acid, Nature, 440, 195, 10.1038/nature04603, 2006.

Stieger, B., Spindler, G., Fahlbusch, B., Müller, K., Grüner, A., Poulain, L., Thöni, L., Seitler, E., Wallasch, M., and Herrmann, H.: Measurements of PM_{10} ions and trace gases with the online system MARGA at the research station Melpitz in Germany – A five-year study, J. Atmos. Chem., 75, 33-70, 10.1007/s10874-017-9361-0, 2018.

Su, H., Cheng, Y. F., Shao, M., Gao, D. F., Yu, Z. Y., Zeng, L. M., Slanina, J., Zhang, Y. H., and Wiedensohler, A.: Nitrous acid (HONO) and its daytime sources at a rural site during the 2004 PRIDE-PRD experiment in China, J. Geophys. Res. Atmos., 113, doi:10.1029/2007JD009060, 2008.

Su, H., Cheng, Y. F., Oswald, R., Behrendt, T., Trebs, I., Meixner, F. X., Andreae, M. O., Cheng, P., Zhang, Y., and Poschl, U.: Soil Nitrite as a Source of Atmospheric HONO and OH Radicals, Science, 333, 1616-1618, 10.1126/science.1207687, 2011.

Tuch, T. M., Haudek, A., Müller, T., Nowak, A., Wex, H., and Wiedensohler, A.: Design and performance of an automatic regenerating adsorption aerosol dryer for continuous operation at monitoring sites, Atmos. Meas. Tech., 2, 417-422, 10.5194/amt-2-417-2009, 2009.

VandenBoer, T. C., Brown, S. S., Murphy, J. G., Keene, W. C., Young, C. J., Pszenny, A. A. P., Kim, S., Warneke, C., de Gouw, J. A., Maben, J. R., Wagner, N. L., Riedel, T. P., Thornton, J. A., Wolfe, D. E., Dubé, W. P., Öztürk, F., Brock, C. A., Grossberg, N., Lefer, B., Lerner, B., Middlebrook, A. M., and Roberts, J. M.: Understanding the role of the ground surface in HONO vertical structure: High resolution vertical profiles during NACHTT-11, J. Geophys. Res. Atmos., 118, 10,155-110,171, doi:10.1002/jgrd.50721,

2013.

VandenBoer, T. C., Markovic, M. Z., Sanders, J. E., Ren, X., Pusede, S. E., Browne, E. C., Cohen, R. C., Zhang, L., Thomas, J., Brune, W. H., and Murphy, J. G.: Evidence for a nitrous acid (HONO) reservoir at the ground surface in Bakersfield, CA, during CalNex 2010, Journal of Geophysical Research: Atmospheres, 119, 9093-9106, 10.1002/2013jd020971, 2014.

VandenBoer, T. C., Young, C. J., Talukdar, R. K., Markovic, M. Z., Brown, S. S., Roberts, J. M., and Murphy, J. G.: Nocturnal loss and daytime source of nitrous acid through reactive uptake and displacement, Nature Geoscience, 8, 55-60, 10.1038/ngeo2298, 2015.

Villena, G., Wiesen, P., Cantrell, C. A., Flocke, F., Fried, A., Hall, S. R., Hornbrook, R. S., Knapp, D., Kosciuch, E., Mauldin III, R. L., McGrath, J. A., Montzka, D., Richter, D., Ullmann, K., Walega, J., Weibring, P., Weinheimer, A., Staebler, R. M., Liao, J., Huey, L. G., and Kleffmann, J.: Nitrous acid (HONO) during polar spring in Barrow, Alaska: A net source of OH radicals?, Journal of Geophysical Research-Atmospheres, 116, 10.1029/2011jd016643, 2011.

Volten, H., Bergwerff, J. B., Haaima, M., Lolkema, D. E., Berkhout, A. J. C., van der Hoff, G. R., Potma, C. J. M., Kruit, R. J. W., van Pul, W. A. J., and Swart, D. P. J.: Two instruments based on differential optical absorption spectroscopy (DOAS) to measure accurate ammonia concentrations in the atmosphere, Atmos. Meas. Tech., 5, 413-427, 10.5194/amt-5-413-2012, 2012.

Wang, J., Zhang, X., Guo, J., Wang, Z., and Zhang, M.: Observation of nitrous acid (HONO) in Beijing, China: Seasonal variation, nocturnal formation and daytime budget, Sci. Total Environ., 587, 350-359, 10.1016/j.scitotenv.2017.02.159, 2017.

Wang, L. M., and Zhang, J. S.: Detection of nitrous acid by cavity ring down spectroscopy, Environ. Sci. Technol., 34, 4221-4227, 10.1021/es0011055, 2000.

Wentworth, G. R., Murphy, J. G., Benedict, K. B., Bangs, E. J., and Collett Jr., J. L.: The role of dew as a night-time reservoir and morning source for atmospheric ammonia, Atmos. Chem. Phys., 16, 7435-7449, 10.5194/acp-16-7435-2016, 2016.

Wiedensohler, A.: An approximation of the bipolar charge distribution for particles in the submicron size range, J. Aerosol Sci., 19, 387-389, https://doi.org/10.1016/0021-8502(88)90278-9, 1988.

Wiedensohler, A., Birmili, W., Nowak, A., Sonntag, A., Weinhold, K., Merkel, M., Wehner, B., Tuch, T., Pfeifer, S., Fiebig, M., Fjäraa, A. M., Asmi, E., Sellegri, K., Depuy, R., Venzac, H., Villani, P., Laj, P., Aalto, P., Ogren, J. A., Swietlicki, E., Williams, P., Roldin, P., Quincey, P., Hüglin, C., Fierz-Schmidhauser, R., Gysel, M., Weingartner, E., Riccobono, F., Santos, S., Grüning, C., Faloon, K., Beddows, D., Harrison, R., Monahan, C., Jennings, S. G., O'Dowd, C. D., Marinoni, A., Horn, H.-G., Keck, L., Jiang, J., Scheckman, J., McMurry, P. H., Deng, Z., Zhao, C. S., Moerman, M., Henzing, B., de Leeuw, G., Löschau, G., and Bastian, S.: Mobility particle size spectrometers: harmonization of technical standards and data structure to facilitate high quality long-term observations of atmospheric particle number size distributions, Atmos. Meas. Tech., 5, 657-685, 10.5194/amt-5-657-2012, 2012.

Wiedensohler, A., Wiesner, A., Weinhold, K., Birmili, W., Hermann, M., Merkel, M., Müller,

T., Pfeifer, S., Schmidt, A., Tuch, T., Velarde, F., Quincey, P., Seeger, S., and Nowak, A.: Mobility particle size spectrometers: Calibration procedures and measurement uncertainties, Aerosol Sci. Technol., 52, 146-164, 10.1080/02786826.2017.1387229, 2018.

Wohlfahrt, G., Sapinsky, S., Tappeiner, U., and Cernusca, A.: Estimation of plant area index of grasslands from measurements of canopy radiation profiles, Agric. For. Meteorol., 109, 1-12, https://doi.org/10.1016/S0168-1923(01)00259-3, 2001.

Wong, K. W., Oh, H.-J., Lefer, B. L., Rappenglück, B., and Stutz, J.: Vertical profiles of nitrous acid in the nocturnal urban atmosphere of Houston, TX, Atmos. Chem. Phys., 11, 3595-3609, 10.5194/acp-11-3595-2011, 2011.

Xu, Z., Liu, Y., Nie, W., Sun, P., Chi, X., and Ding, A.: Evaluating the measurement interference of wet rotating-denuder–ion chromatography in measuring atmospheric HONO in a highly polluted area, Atmos. Meas. Tech., 12, 6737-6748, 10.5194/amt-12-6737-2019, 2019.

Ye, C., Gao, H., Zhang, N., and Zhou, X.: Photolysis of Nitric Acid and Nitrate on Natural and Artificial Surfaces, Environ. Sci. Technol., 50, 3530-3536, 10.1021/acs.est.5b05032, 2016.

Yu, Y., Galle, B., Panday, A., Hodson, E., Prinn, R., and Wang, S.: Observations of high rates of NO_2-HONO conversion in the nocturnal atmospheric boundary layer in Kathmandu, Nepal, Atmos. Chem. Phys., 9, 6401-6415, 10.5194/acp-9-6401-2009, 2009.

Zhang, B., and Tao, F.-M.: Direct homogeneous nucleation of NO_2, H_2O, and NH_3 for the production of ammonium nitrate particles and HONO gas, Chem. Phys. Lett., 489, 143-147, 10.1016/j.cplett.2010.02.059, 2010.

Zhang, L., Wang, T., Zhang, Q., Zheng, J., Xu, Z., and Lv, M.: Potential sources of nitrous acid (HONO) and their impacts on ozone: A WRF-Chem study in a polluted subtropical region, J. Geophys. Res. Atmos., 121, 3645-3662, doi:10.1002/2015JD024468, 2016.

Zhou, X., Gao, H., He, Y., Huang, G., Bertman, S. B., Civerolo, K., and Schwab, J.: Nitric acid photolysis on surfaces in low-NOx environments: Significant atmospheric implications, Geophys. Res. Lett., 30, 10.1029/2003gl018620, 2003.

Zhou, X., Huang, G., Civerolo, K., Roychowdhury, U., and Demerjian, K. L.: Summertime observations of HONO, HCHO, and O_3 at the summit of Whiteface Mountain, New York, J. Geophys. Res. Atmos., 112, doi:10.1029/2006JD007256, 2007.

Zhou, X., Zhang, N., TerAvest, M., Tang, D., Hou, J., Bertman, S., Alaghmand, M., Shepson, P. B., Carroll, M. A., Griffith, S., Dusanter, S., and Stevens, P. S.: Nitric acid photolysis on forest canopy surface as a source for tropospheric nitrous acid, Nature Geoscience, 4, 440-443, 10.1038/ngeo1164, 2011.

Table 1. Mean and mean error as 2 times the standard deviation of the measured HONO (LOPAP) and the other pollutants in the Melpitz station during daytime (D, 04:00-18:00, UTC) and nighttime (N, 18:00-04:00, UTC).

	D	N		D	N
NO (ppbv)	1.0 ±0.5	0.5 ±0.3	HCl (ppbv) [b]	0.02 ±0.03	0.01 ±0.01
NOx (ppbv)	4 ±1	6 ±2	HNO_3 (ppbv) [b]	0.2 ±0.1	0.2 ±0.1
NO_2 (ppbv)	3 ±1	5 ±2	NH_3 (ppbv) [b]	17 ±7	8 ±4
HONO (pptv)[a]	162 ±96	254 ±114	Cl^- (μg m^{-3}) [b]	0.03 ±0.04	0.01 ±0.01
O_3 (ppbv)	36 ±7	19 ±13	NO_3^- (μg m^{-3}) [b]	3 ±2	2 ±1
SO_2 (ppbv)	0.8 ±0.4	0.5 ±0.3	SO_4^{2-} (μg m^{-3}) [b]	1.4 ±0.5	1.3 ±0.6
T (℃)	16 ±3	11 ±5	Na^+ (μg m^{-3}) [b]	0.02 ±0.03	0.01 ±0.01
RH (%)	67 ±7	85 ±11	NH_4^+ (μg m^{-3}) [b]	1.1 ±0.7	0.8 ±0.4
Wind speed (m s^{-1})	3 ±2	1.2 ±0.7	K^+ (μg m^{-3}) [b]	0	0.001 ±0.002
HONO/NOx (%)	0.04 ±0.02	0.05 ±0.02	Mg^{2+} (μg m^{-3}) [b]	0.03 ±0.01	0.02 ±0.04
NO/NOx (%)	0.3 ±0.1	0.1 ±0.1	Ca^{2+} (μg m^{-3}) [b]	0.2 ±0.1	0.2 ±0.1
OH (molecule cm^{-3})	(2.8 ±0.7) ×10^6		NO_2^- (μg m^{-3}) [b]	0.01 ±0.01	0.03 ±0.02

[a] HONO derived from LOPAP;

[b] data obtained from the MARGA instrument

Table 2. Nitrite concentration measured in dew water.

Date 2019	Plate number	Initial hour (UTC)	Final hour (UTC)	Volume (ml)	Blank NO_2^- ($\mu g\ L^{-1}$) [a]	Final NO_2^- ($\mu g\ L^{-1}$) [b]	F_{NO2-} ($\mu g\ m^{-2}$)	pH [c]
May 8th	1	18:00	5:25	76.60	0.0018	41.87	2.10	6.40
	2		5:45	75.60	0.0017	42.84	2.20	6.45
May 11th	1	18:00	3:20	94.00	0.0055	128.23	8.00	7.00
	2		4:20	80.00	0.0005	120.43	6.40	6.90
	1	3:30	5:20	13.00	0.0006	164.62	1.43	7.00
May 13th	1	18:00	4:45	72.00	0.0001	43.87	2.10	6.30
	2		5:20	79.00	0.0001	58.81	3.10	6.40
May 14th	1	18:00	5:00	15.00	0.0001	148.90	1.50	6.80
	2		5:00	21.00	0.0001	91.44	1.30	6.70

[a] note that the blank NO_2^- concentration is below the detection limit of 0.02 $\mu g\ L^{-1}$.

[b] Final NO_2^- = Raw NO_2^- - Blank NO_2^-

[c] pH was measured by a pH meter on a subsample of the total volume

Table 3. The ratio $HONO_{corr}/NO_2$ and the NO_2-HONO conversion frequency during nighttime.

Date	UTC	R^2	$HONO_{corr}/NO_2$	k_{het} (h^{-1})
19/04/2018	17:30-19:50	0.45	0.118 ±0.010	0.043 ±0.002
21/04/2018	18:20-20:30	0.64	0.055 ±0.004	0.012 ±0.002
22/04/2018	18:10-21:20	0.79	0.161 ±0.005	0.030 ±0.002
25/04/2018	17:31-21:20	0.69	0.061 ±0.003	0.010 ±0.001
27/04/2018	18:00-23:41	0.48	0.113 ±0.006	0.016 ±0.001
28/04/2018	18:00-19:50	0.44	0.152 ±0.008	0.050 ±0.004
			0.110 ±0.041	0.027 ±0.017

Table 4. Summary of the temporary HONO emission rate from dew water, $k_{emission}$ from April 19th to 29th, 2018.

Period	$k_{emission}$ (pptv $\%^{-1}$ s^{-1})	
	Min	Max
21/4/2018	0.0054	0.0357
22/4/2018	0.0048	0.0314
24/4/2018	0.0057	0.0192
26/4/2018	0.0067	0.0302
27/4/2018	0.0048	0.0215
28/4/2018	0.0079	0.017
Average	0.006 ±0.001	0.026 ±0.008

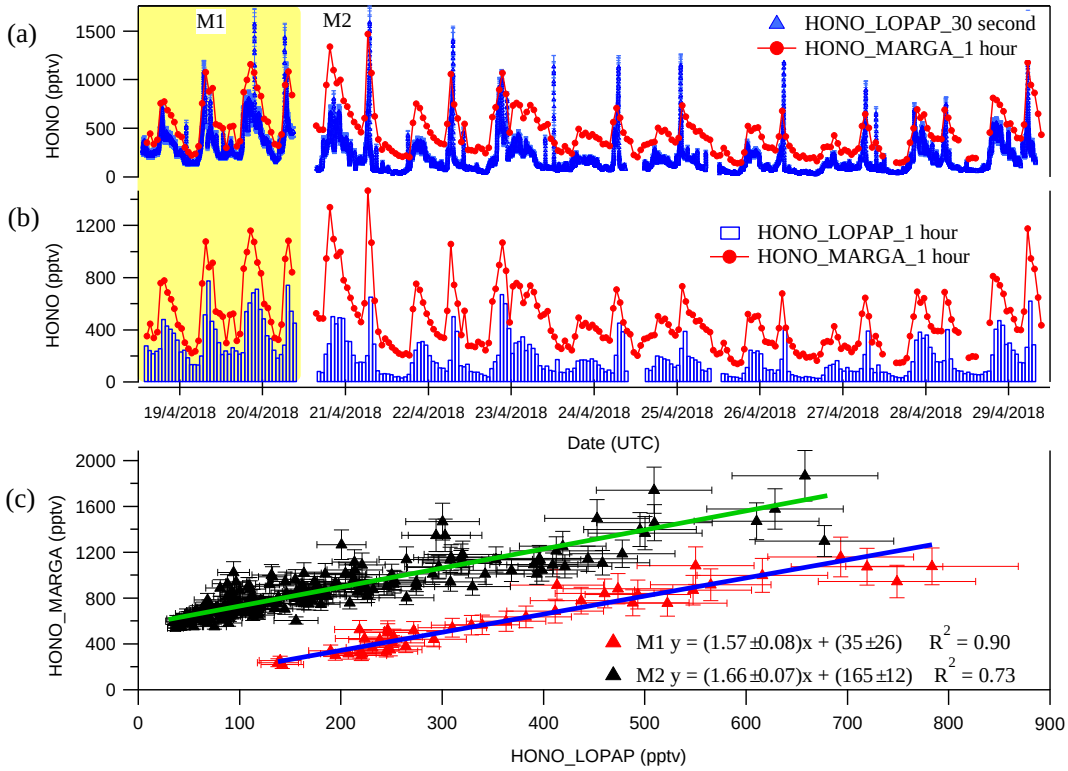

Figure 1. Time courses of HONO as hourly measured by MARGA and 30 seconds measured by LOPAP (a) and normalized hourly for LOPAP (b). (c) blue and green lines represent the error weighted orthogonal regression analysis between MARGA and LOPAP for two different comparison period of M1 and M2, respectively. The error bar in the panel (c) indicates the measurement error of HONO concentrations in LOPAP and MARGA. The HONO concentration of MARGA in panel (c) is shifted 400 pptv for clarity.

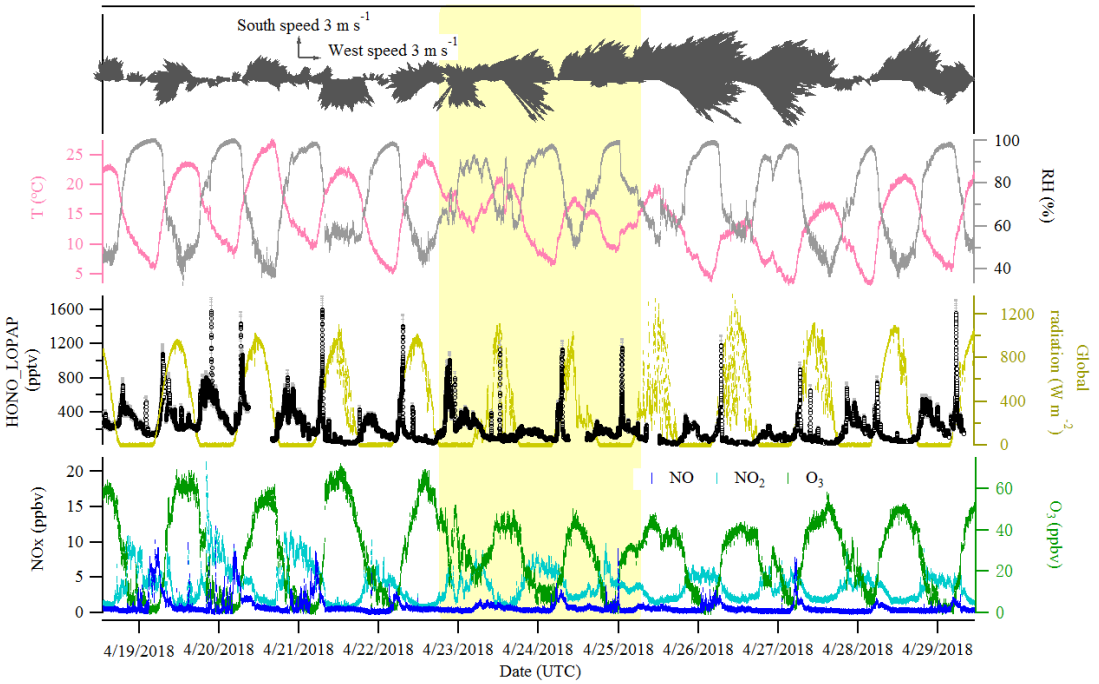

Figure 2. Time series of HONO (LOPAP measurement), NO, NO_2, O_3, global radiation, temperature (T), relative humidity (RH) and surface wind in Melpitz from April 19th to 29th, 2018. The gaps were mainly due to the maintenance of the instruments. The yellow shadow indicates two sets of observations discussed in section 3.3. The gray color in the HONO panel indicates the measurement error of HONO concentrations.

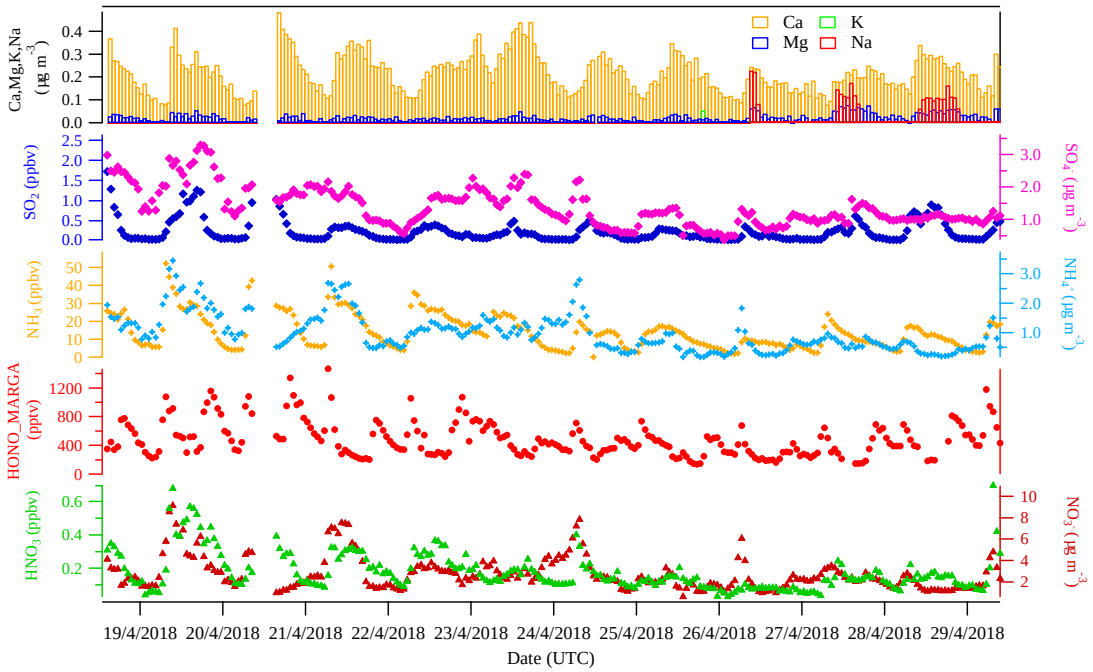

Figure 3. The hourly time-resolved quantification of water-soluble ions in PM_{10} (NO_3^-, SO_4^{2-}, NH_4^+, Na^+, K^+, Mg^{2+}, Ca^{2+}) and their corresponding trace gases (HONO, HNO_3, SO_2, NH_3) were measured by MARGA in Melpitz from April 19th to 29th, 2018.

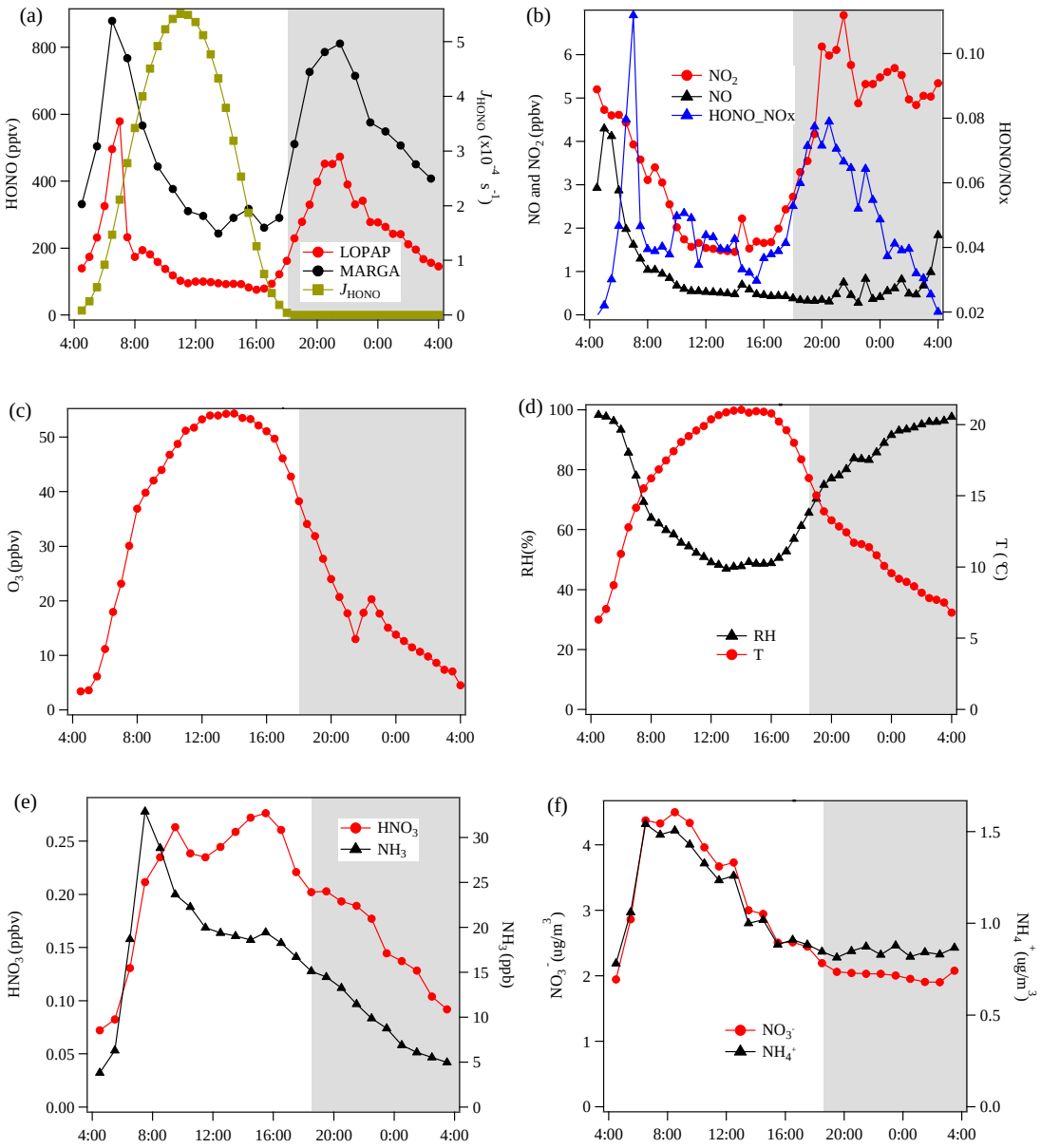

Figure 4. Diurnal variations of HONO and related species during the measurement period except for two sets of observations show in Figure 5 at Melpitz site. The photolysis rate of HONO was obtained from the TUV model. The grey shaded area indicates the nighttime period (18:00-04:00 UTC).

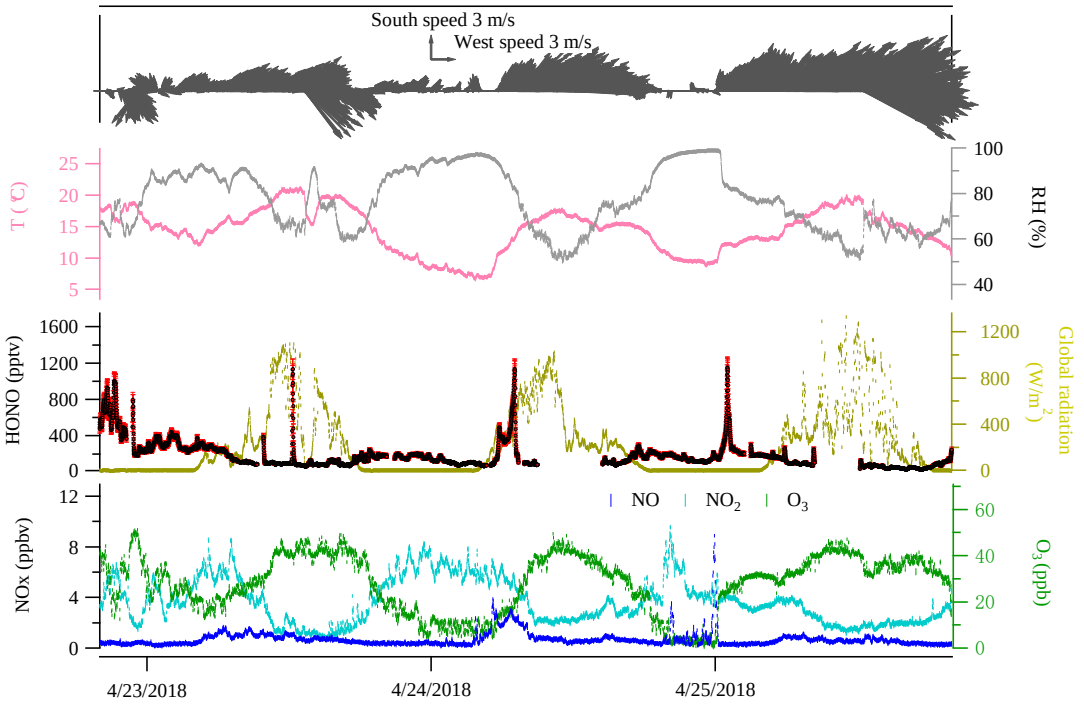

Figure 5. Case events for HONO (LOPAP) and related species at Melpitz site during the day April 23rd to 25th, 2018. The red color in the HONO panel indicates the measurement error of HONO concentrations.

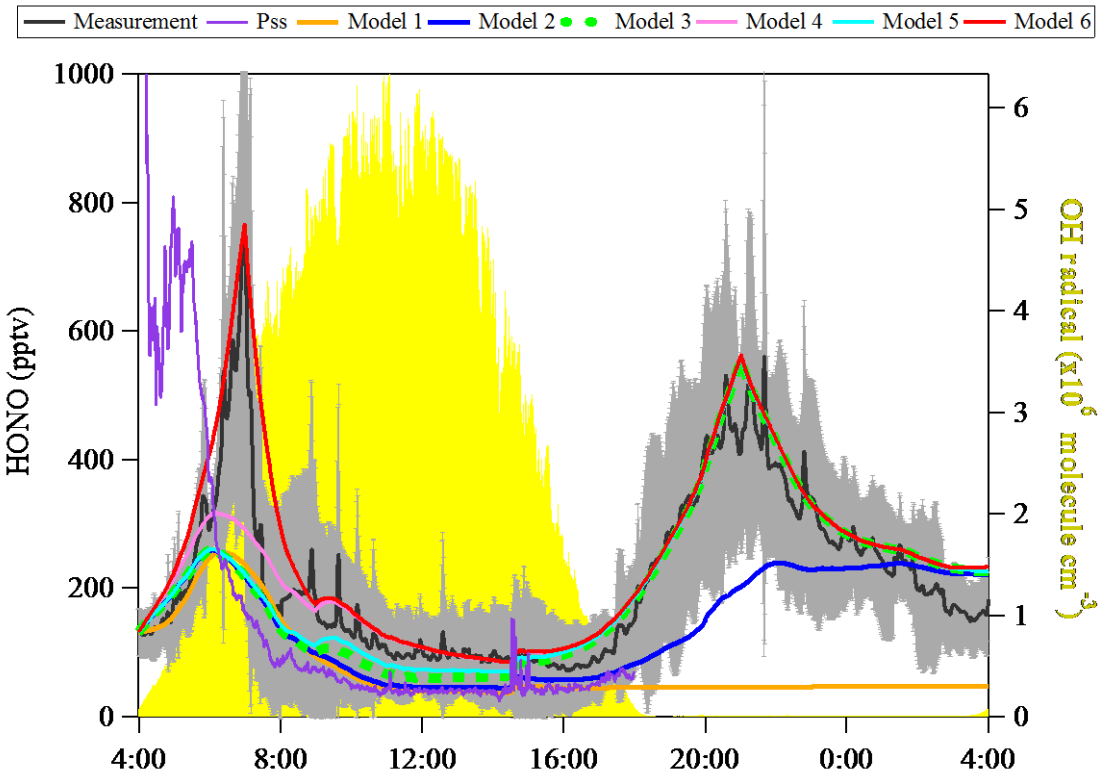

Figure 6. Observed average HONO atmospheric concentration (black line, +-1σ in shaded area) and the model calculated HONO concentration including different HONO production and loss processes. Pss presents model results by assuming an instantaneous photo-equilibrium between the gas-phase formation (R7) and gas-phase loss processes (R1 and R11) of HONO; Model 1 includes R1+R7+R11. Model 2 includes R1+R2+R7+R11+surface deposition (00:00-00:00), whereas Model 3 describes R1+R2+R7+R11+surface deposition (17:00-8:00). And Model 3 is used to be the base to investigate the effect of R9 (Model 4), R5 (Model 5) and the combination of R5+R9+Dew HONO emission (4:30-7:00) (Model 6).

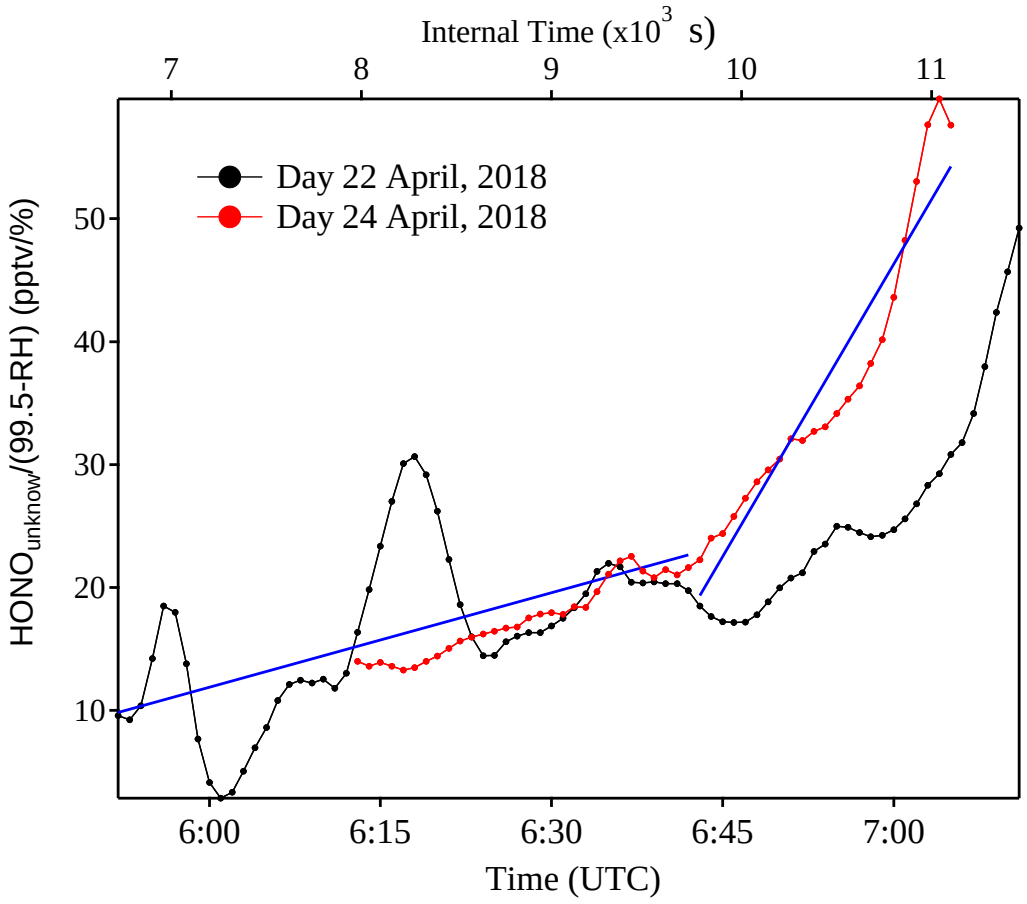

Figure 7. Example of $\frac{HONO_{unknown}}{99.5-RH}$ as a function of time (zero point from time 4:30, UTC) to estimate the temporary HONO emission rate from dew water ($k_{emission}$). Blue line is the linear least-square analysis of $\frac{HONO_{unknown}}{99.5-RH}$ vs. internal time to obtain the minimum and maximum of $k_{emission}$, respectively.

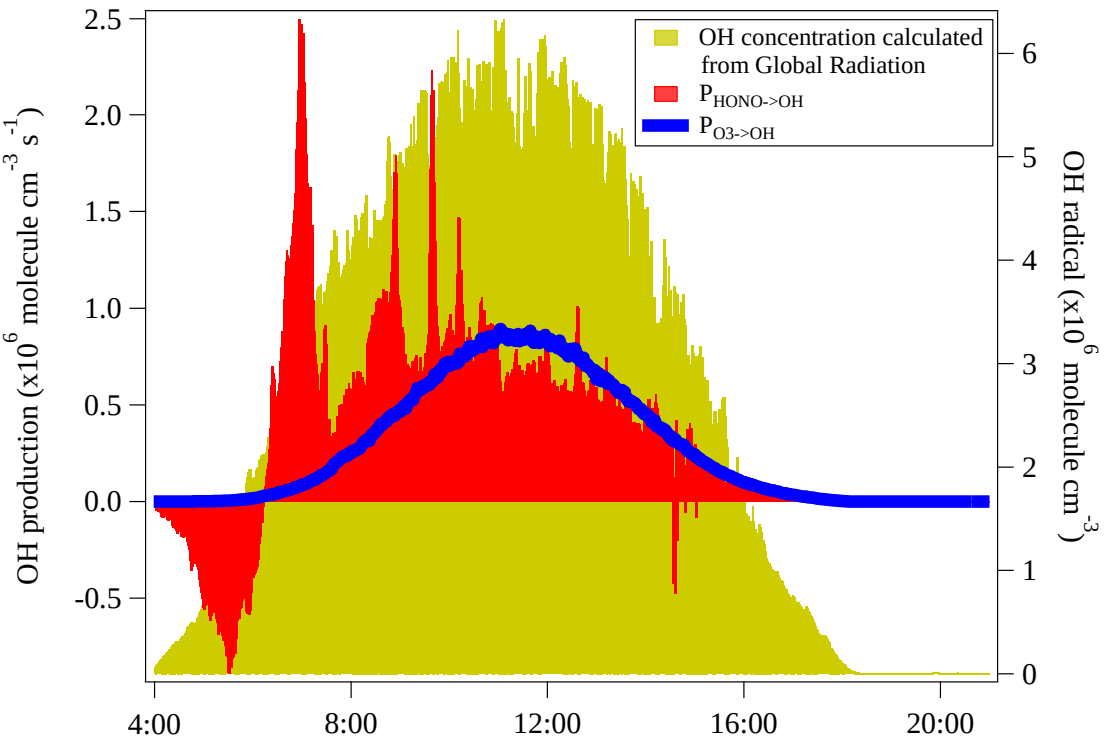

Figure 8. The OH production rates from photolysis of HONO and O_3 in Melpitz station from April 19th to 29th, 2018. The OH concentration is also shown as yellow area plot, which was calculated from the global radiation flux measurement: [OH]=A*Rad taken from Größ et al. (2018).